UC Irvine
UC Irvine Previously Published Works

Title

The Measurement and Analysis of Heterogeneous Emissions by Multifrequency Phase and Modulation Fluorometry

Permalink

Journal

ISSN

Authors

Jameson, David M
Gratton, Enrico
Hall, Robert D

Publication Date

1984

DOI

Copyright Information

Peer reviewed

The Measurement and Analysis of Heterogeneous Emissions by Multifrequency Phase and Modulation Fluorometry

DAVID M. JAMESON
Department of Pharmacology
The University of Texas Health Science Center at Dallas
Dallas, Texas 75235

ENRICO GRATTON
Department of Physics
University of Illinois at Urbana-Champaign
Urbana, Illinois 61801

ROBERT D. HALL
Laboratory of Molecular Biophysics
National Institute of Environmental Health Sciences
Research Triangle Park
North Carolina 27709

I. INTRODUCTION*

A. Statement of the Problem

During the last few decades fluorescence spectroscopy has developed into an important and widely used technique in the physical, chemical, and biological sciences. The increasing sophistication of theory and methodology has permitted us to apply fluorescence techniques profitably to a variety of complex problems. A fundamental consideration in the spectroscopic analysis of any system is the degree of sample heterogeneity. We wish to know, for example, if the heterogeneity arises from a melange of fluorophores (this condition often reduces to the question of sample purity) as a consequence of solvent-fluorophore interactions or from the fluorophore per se. An exact quantitation of

---

*Abbreviations. DENS: 2,5-Diethylaminoethylnaphthalenesulfonate. DPH: 1,6-Diphenyl-1,3,5-hexatriene. POPOP: p-Bis(2-(5-phenyloxazo-1yl))benzene. 9-CA: 9-Carboxy-anthracene. 9-10-DPA: 9,10-Diphenyl-anthracene.

the nature and extent of the heterogeneity may be critical to our under-
standing of the origins of that phenomenon. These data have important
implications whether the desired information concerns a compositional
description for analytical purposes or whether the fluorophore is de-
signed to probe the molecular environment.

The extent of heterogeneity may not be apparent from observation
of the spectral distribution or polarization of the emission. Fluorophores
exhibiting very similar emission or excitation spectra may differ mark-
edly in their lifetimes. Hence time domain measurements offer a power-
ful means of examining and quantitating heterogeneous emissions.

The fluorescence lifetime can be expressed as the reciprocal of the
radiative rate process, k_r. The observed relative fluorescence inten-
sity, I, of a system will be related to the radiative (k_r) and nonradiative
(k_{nr}) processes according to

$$I = k_r/(k_r + k_{nr}) \tag{1}$$

In this greatly simplified expression we lump together the various mech-
anisms which may deactivate the excited state such as internal conver-
sion, energy transfer, and chemical quenching. Exact knowledge of the
lifetime may be required for the correct interpretation of many obser-
vations related to the intrinsic photophysics of optical probes and their
behavior in complex systems such as biological milieu. The correct
physical interpretation of results on quantum yields, polarizations, and
quenching rate constants, for example, depend upon knowledge of the
fluorescence lifetime. Several excellent discussions of the pertinence
of lifetime data have appeared [1-4].

B. Measurement of Fluorescence Lifetimes

1. Impulse Response

The measurement of fluorescence lifetimes is generally accom-
plished by either an impulse response or a harmonic response tech-
nique. With the impulse response technique the illumination function is
a pulse of light of short duration, ideally a delta function. Such pulses
are traditionally generated by flashlamps [2], pulsed lasers [5], and
more recently by synchrotron radiation sources [6, 7]. The direct
decay curve, that is, the record of fluorescence intensity versus time,
is obtained by using detectors with temporal resolution such as streak
cameras, time sampling circuitry or, most commonly, the time corre-
lated single photon counting approach [2, 3]. If the fluorescence lifetime
is monoexponential and long compared to the exciting pulse duration
and if the distortion of the pulse shape by the detecting elements is

negligible, then the data analysis is straightforward. In cases where
the exciting pulse duration is not negligible compared to the fluores-
cence lifetime, then the fluorescence decay curve will be distorted
by the excitation function and a deconvolution procedure must be used
to extract the time decay curve. Furthermore, if the emission is
characterized by two or more decay times, then the data must be fit
by the appropriate decay rates and their preexponential factors. The
observed decay curves will thus take the form

$$I(t) = \sum_i \alpha_i e^{-t/\tau_i} \tag{2}$$

where I(t) is the fluorescence intensity at time t after excitation, α_i is
the amplitude of the i-th component, and τ_i is the lifetime of the i-th
component. Critical analysis of a number of deconvolution and data fit-
ting routines have been given [8-10].

2. Harmonic Response

    In the traditional harmonic response approach the sample is illumi-
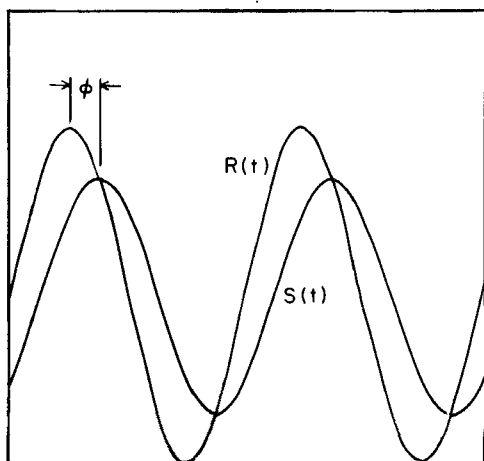nated by a light source with an intensity which is sinusoidally modulated

FIG. 1. Schematic representation of the excitation R(t) and fluores-
cence S(t) waveforms. The fluorescence is delayed by an angle ϕ with
respect to the excitation.

at high frequencies, typically in the megahertz range. In such a case
the fluorescence intensity will also be modulated sinusoidally at the
excitation frequency but will be delayed by a phase angle, ϕ, due to the
finite persistence of the excited state, a situation depicted in Fig. 1.
Additionally, the relative modulation, that is, the effective ac/dc ratio
of the fluorescence, will be less than that of the exciting light. This
demodulation forms the basis of a lifetime measurement independent
of the phase shift. In this review we shall consider primarily the instru-
mentation required to realize the modulation of the exciting light and to
effect the phase and modulation measurements as well as the appropri-
ate data analysis procedures. We shall anticipate our discussion by
emphasizing that the availability of true multifrequency instrumentation
has added a new dimension to phase and modulation fluorometry and has
allowed the method to realize its true potential.

II. INSTRUMENTATION

A. Brief History

The literature on phase fluorometry is considerable. A thorough
account of the development of phase fluorometry up until 1966 has been
written by Birks and Munro [1]. A more recent discussion of phase
fluorometry up until 1980 has been penned by Teale [11]. We shall only
outline some of the major developments in this area and refer readers
with a sustaining interest to the aforementioned articles and to the
original literature for detailed discussions. The first phase fluorometer
appears to be that of Gaviola [12], built in 1926, although certain as-
pects of the problem were anticipated by Abraham and Lemoine [13] in
1899. Gaviola's instrument utilized the Kerr effect to modulate the light
intensity and relied upon visual detection of the fluorescence. The fol-
lowing decades brought a number of diverse approaches to the light
modulation and detection systems. The ultrasonic diffraction grating
was utilized by Maercks [14] and Tumerman and Szymanowski [15] while
photomultipliers were introduced in this area of research by Ravilious
et al. [16]. Noteworthy advances were also made by Bailey and Rollefson
[17], Birks and Little [18], Muller et al. [19], Schmillen [20], Bauer
and Rozwadowski [21], and Spencer and Weber [22].
    Modulation measurements really began seriously with the instru-
ments of Hamilton [23], Birks and Dyson [24], and Spencer and Weber
[22]. The notion of using cross-correlation techniques to move the
measurement to the low frequency domain with subsequent improvement
in stability was introduced by Schmillen [20] although his particular
approach did not fully realize the potential of the method. Birks and

Little [18] modulated the photomultiplier's response with the same fre-
quency used to excite the sample. Spencer and Weber [22] extended
this cross-correlation approach by adding a variable low frequency
component to the main frequency and modulating the photomultiplier's
response with this new frequency (see Appendix 3).

The phase fluorometers mentioned above were essentially single
(or at best two) frequency instruments, moreover modification of the
operating frequency was not generally a simple and rapid procedure.
True multifrequency operation has been developed only recently and is
characterized by the ability to modulate the light at arbitrary frequencies
rapidly without recourse to additional instrument adjustment.

B. State of the Art

1. General

In the last few years a number of research groups have published
descriptions of new phase fluorometers. These instruments include
those by Haar and Hauser [25], Saleem and Rimai [26], Gugger and
Calzaferri [27, 28], Hieftje et al. [29], Menzel and Popovic [30],
Merkelo et al. [31], Lytle et al. [32], Ide et al. [33], and Gratton and
Limkeman [34]. These instruments differ in their approach to the
strategies for light modulation and signal detection and processing but
all utilize a CW laser for the sample excitation. As we shall discuss
later, synchrotron radiation is also now being utilized for phase
fluorometry.

2. Commercial Instrumentation

To our knowledge the only commercially available phase fluorome-
ter is in the SLM 4800 series. Since many researchers in the biophys-
ical and biochemical sciences utilize this instrument, we shall discuss
a few of the more important operational principles in some detail.
Some additional components are described in the section concerning
the multifrequency instruments (Sec. II-B-3).

In the SLM 4800A instrument the light from a 450-W xenon arc
passes through the excitation monochromator and is then intensity
modulated at either 6, 18, or 30 MHz before impinging upon the sample.
The light modulation principle is the Debye-Sears [35] effect which is
realized with an ultrasonics tank placed after the excitation mono-
chromator. Ultrasonic waves are generated in a stainless steel tank
containing a liquid (typically 19% ethanol in water to minimize the tem-
perature dependence of the sound velocity) by a transducer, an x-cut
piezoelectric quartz crystal, mounted in an aluminum or stainless-steel
cylinder. Proper orientation of a reflector situated at the opposite end

of the tank establishes an ultrasonic standing wave in the solution. The standing waves are formed when the length of the acoustic path is a multiple of half a wavelength of the ultrasonic wave. These standing waves create planes of higher refractive index which collapse and form with the ultrasonic waves. Incident plane waves of light will respond as they do toward an ordinary low order diffraction grating and an inter- mittent interference pattern will form and collapse following the condi- tion of the standing wave. The crystal face and the reflecting surface must be adjusted to parallel orientation with micrometers (on the re- flector mount) to insure the standing wave. Additionally, since the wavelength of the acoustic wave in water is short (100 μm at 15 MHz) and since the width of the acoustic resonance peak is on the order of 2-5 kHz (at 15 MHz), the length of the tank must also be slightly adjusted in order to achieve the resonance condition at a constant frequency. The length of the ultrasonics path is approximately 5 cm which corresponds to an acoustic resonance every 15 kHz. In this geometrical condition the width of the resonance is on the same order of magnitude as the difference between two adjacent resonances which means that exciting one mode exclusively is difficult. The tuning of the tank is achieved by successively adjusting the orientation of the reflector with respect to the crystal and then adjusting the distance between these two components until a maximum modulation value is reached. When standing waves are obtained, modulation of the light at twice the exciting frequency occurs. The modulation is detected by an ac meter, and when the tank is per- fectly tuned the modulation of the exciting light, that is, the ac/dc ratio, should, given the particular amplifier gain characteristics utilized, reach a value of about 2. The degree of modulation attained depends strongly, however, on the parallelism of the exciting light passing through the tank and good modulation can be reached only with narrow excitation slits. In addition, more than one mode of modulation may exist in the tank which can result in artifacts which we shall discuss presently.

The modulation frequencies of 6, 18, and 30 MHz result from the fundamental, 3rd, and 5th harmonic of the piezoelectric crystal. We should note that in principle a Debye-Sears tank permits modulation at many frequencies. In practice the lower frequency is limited by the details of the tank's construction and modulation frequencies less than 1 MHz are difficult to achieve. The high frequency limit is imposed by the absorption of sound in the tank medium and by the stringent require- ment for parallelism between the crystal and reflector. The practical upper limit at present is less than 100 MHz.

The emitted light (or scattered light from a scattering solution which can be interposed in the same position as the sample) is detected by a photomultiplier, the last dynode of which is modulated at a frequency

equal to the light modulation frequency (6, 18, or 30 MHz) plus a small additional frequency (typically 25 Hz). This procedure, cross-correlation (see Appendix 3), offers advantages over direct rf measurements in terms of accuracy and noise considerations. Essentially, the phase and modulation information of the signal is transposed to the low frequency range where digital averaging techniques can be easily implemented. The cross-correlation frequency is obtained by an electronic phase shifting method developed by one of us (E.G.), called the digital phase shifter. The digital phase shifter is simple and inexpensive and the version present in the SLM instrument can be used in principle over the modulation range of 1 to 60 MHz (see Appendix 5). The phase delay and demodulation of the emission relative to the scattered light is then calculated as discussed in the following section.

    Standard photomultipliers utilized on the SLM instrument include the EMI 9813QB and the Hamamatsu R928. Although the EMI 9813QB is a high sensitivity tube, it has the disadvantage of demonstrating a severe color error, an artifact which will be discussed later on. (We shall note that on recent models a modified 9813QB photomultiplier with improved characteristics is used.) The precision of lifetime measurements on a standard SLM instrument is on the order of 100 to 200 ps depending upon the signal strength and the experience of the operator. The most important factor which limits the precision of the instrument is undoubtably the stability of the ultrasonics tank. Although the precision of the present commercial phase and modulation instrument is inferior to that of the more sophisticated, homebuilt apparatus described below, its performance compares favorably to that of commercially available pulse lifetime systems. Certainly, the introduction of the commercial phase and modulation fluorometer in the early 1970s was an important step in the general renewal of interest in phase fluorometry.

3. Research Instrumentation

    We shall now discuss in some detail a variable frequency cross-correlation phase fluorometer. This instrument, recently described [34], operates over the frequency range of 1 to 160 MHz with a time resolution of several picoseconds. The basic instrument layout is shown in Fig. 2. The light source is an argon ion laser (Spectra Physics Model 164/9) equipped with selective prism wavelength and UV optics. An extra-cavity electrooptical element (Pockels cell, Lasermetrics Model LM1) driven by an rf power amplifier (Electronic Navigation Industries Model 411AL 10W) accomplishes the sinusoidal modulation of the light intensity. Two frequency synthesizers (Rockland Model 5600 and Fluke Model 6160A) generate the sinusoidal signals to drive the Pockels cell and modulate the photomultipliers. Both synthesizers are
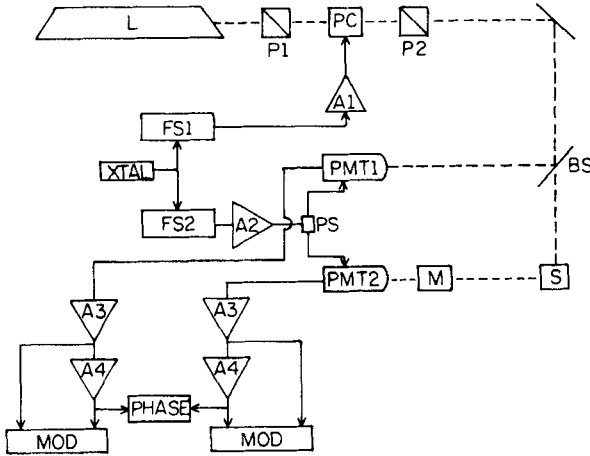
FIG. 2. Block diagram of the laser based cross-correlation phase fluorometer of Ref. 34. L, argon ion laser; A1, 10-W rf power amplifier; A2, 2-W rf power amplifier; XTAL, 10-MHz quartz oscillator; FS1 and FS2, frequency synthesizers; PS, power splitter; PMT1 and PMT2, photomultipliers; M, monochromator; BS, beam splitter; S, sample; A3, preamplifier; A4, ac tuned amplifier; PHASE, phase meter; MOD, modulation meter.

used in the frequency range of 1 to 160 MHz and have a resolution of 1 Hz. Phase coherence of the two signals over the entire frequency range is accomplished by locking the Rockland synthesizer to the Fluke's quartz crystal.

Before entering the Pockels cell the laser beam passes through a calcite prism polarizer which assures complete polarization of the light and establishes a polarization angle of 55° to the vertical laboratory axis. This angle corresponds to the "magic angle" of Spencer and Weber [36] which eliminates errors in the measured lifetime due to Brownian diffusion of the fluorophore. A polarizer placed after the Pockels cell is oriented at 90° to the polarization plane of the first polarizer while the x-axis of the Pockels cell is set at 45° with respect to both polarizers. The Pockels cell is set in a gimbal mounting to facilitate positional adjustments. Application of a voltage across the Pockels cell results in rotation of the plane of polarization of the incident light which may then be passed by the second polarizer. The biasing voltage for the Pockels cell is chosen to insure that the light modulation frequency is equal to the rf driving frequency.

The sample compartment and part of the optical path for this apparatus consists of the Model DP450 optical module from SLM-AMINCO, Urbana, Illinois. The lenses in the excitation path of this module were removed for operation with the laser. The incident light is split by a quartz plate and a fraction of the light is sent to a cuvette containing a scattering solution which is monitored by a reference photomultiplier (Hamamatsu R928). The intensity of the reference signal may be adjusted using neutral density filters. The fluorescent sample and a scattering sample or reference compound are placed in a thermostated rotating turret assembly. The emitted or scattered light is collected and focused on the entrance slit of a Jarrel-Ash 1/4 meter grating monochromator mounted vertically to align the slits parallel to the propagation direction of the incident laser beam to enhance the light collection.

The emission photomultiplier generally utilized is the Hamamatsu R928 which has the advantage of exhibiting no sensible color error (see Section IV-B) and a modest voltage requirement for rf modulation. The photomultiplier output can be varied by 90% with a variation of about 10 V on the last dynode which corresponds to a power of 0.25 W on 50 ohms. An rf amplifier (model 502C from RF Power Labs) supplies this voltage. The frequency of the modulated voltage sent to the last dynode of the photomultiplier is set at 31 Hz above the frequency sent to the Pockels cell. This small frequency difference accomplishes the cross-correlation discussed in Appendix 3.

Two identical detection electronic systems are used to analyze the outputs of the reference and sample photomultipliers. Each channel consists of an ac and a dc amplifier (SLM-AMINCO, Urbana, Illinois). The dc amplifier provides two output signals: an integrated signal proportional to the average intensity (the dc voltage) monitored by a digital voltmeter and a low impedance sinusoidal signal which is input to the ac amplifier. The ac amplifier, tuned at 31 Hz with a Q of 200, has three outputs. One output corresponds to the sinusoidal filtered signal at 31 Hz which can be used with a digital phase sensitive detector (see Section V). Another output is the rectified value of the ac signal (the ac voltage) which is monitored by a digital voltmeter. The third output consists of a square wave used for phase measurements which is generated by the zero crossing of the ac signal. An integrating digital voltmeter displays either the dc signal, the ac signal, or the ac/dc ratio which represents the modulation of the signal.

In a typical measurement the phase delay and modulation ratio for scattered light (from glycogen or a suspension of latex particles) and the fluorescence are obtained relative to the reference photomultiplier or internal reference signal. The absolute phase delay of the fluorescence, ϕ, is then given as

$$\phi = (\phi_R - \phi_F) - (\phi_R - \phi_S) \tag{3}$$

where ϕ_R represents the phase of the internal electronic reference
signal (or the signal from the reference photomultiplier) and ϕ_F and ϕ_S
represent the measured phase readings for the fluorescent and scat-
tered signals, respectively. The phase angle is measured in degrees
with a resolution of 0.01° over the entire frequency range; typically an
integration period of 10 s is utilized. The modulation of the fluorescence,
M, is defined as

$$M = (ac/dc)_F/(ac/dc)_S \tag{4}$$

where the suffixes F and S refer to fluorescence and scattering and the
ac/dc ratio has been described earlier.

The frequency may be changed in seconds merely by entering the
desired frequency into the synthesizers—no additional adjustments on
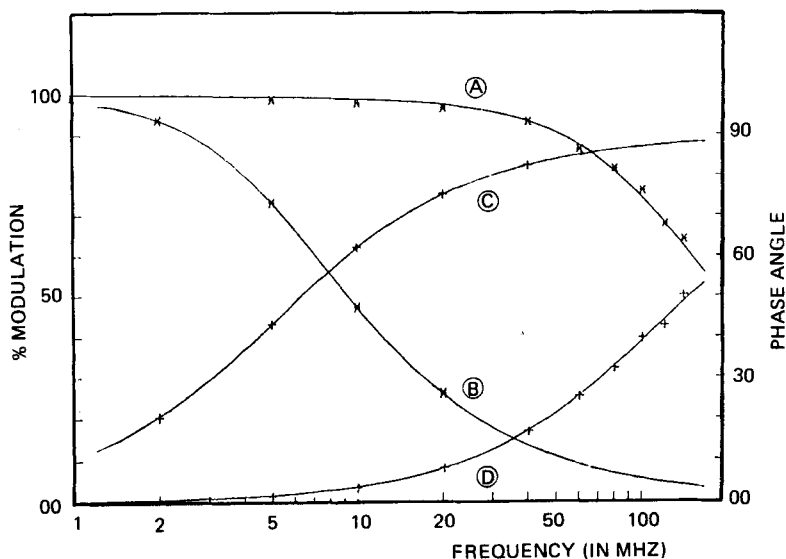the Pockels cell are required. The phase and modulation data at a

FIG. 3. Multifrequency measurements of phase and modulation.
Modulation (A) and phase (D) of POPOP in methanol (τ = 1.38 ns).
Modulation (B) and phase (C) of DENS in water (τ = 29.28 ns). Solid
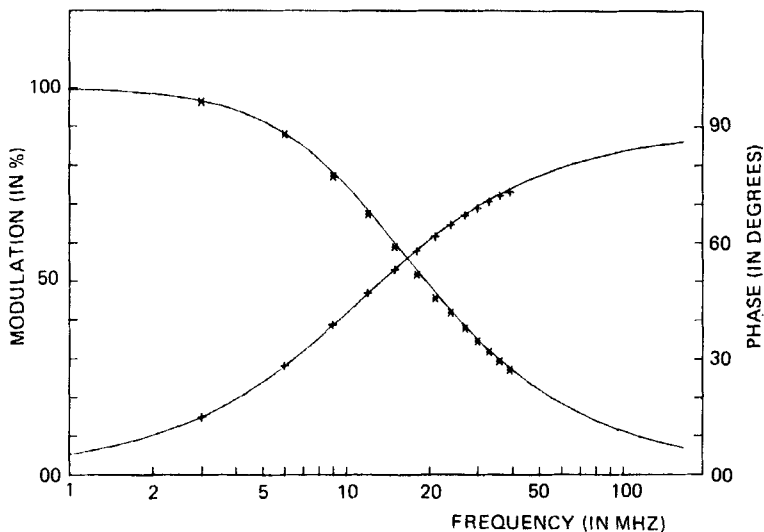curves correspond to single exponential decays.

FIG. 4. Multifrequency measurement of phase and modulation for proptoporphyrin-IX in dioxan. Modulation (*) and phase (+). Solid curves correspond to a single exponential decay, $\tau = 14.14$ ns.

number of frequencies may be entered into a program written for an Apple II computer which plots the data points and various curve fits as shown in Figs. 3 and 4, for example. Details of the heterogeneity analysis typically used will be presented in a following section.

III. DATA ANALYSIS

A. Single Exponential Decay

The theory of the phase fluorometer has been given in detail by Dushinsky [37] who demonstrated that a fluorescent species can be illuminated by light modulated at circular frequency ω according to the expression

$$E(t) = E_0(1 + M_E \sin (\omega t)) \tag{5}$$

where M_E is a modulation factor. In this case the fluorescence due to a population decaying according to a single exponential, $e^{-t/\tau}$, where τ is the lifetime, is given by

$$F(t) = F_0(1 + M_F \sin (\omega t + \phi)) \tag{6}$$

where

$$\tan \phi = \omega \tau \tag{7}$$

and

$$\cos \phi = M = (1 + (\omega \tau)^2)^{-\frac{1}{2}} \tag{8}$$

where M is defined as the relative modulation and corresponds to the ratio of the modulation of the fluorescence to the modulation of the excitation (Eq. 4). One may thus determine the lifetime either by measurement of the phase delay or the relative modulation of the exciting light as illustrated in Fig. 1. For a homogeneous emitting population these two measurements of the lifetime must be equal and independent of the modulation frequency of the measurement. We give in Appendix 1 a derivation of the Dushinsky relations.

B. Multiexponential Decays

1. General

Should the emission be characterized as multiexponential or nonexponential, then the expressions for the single exponential decay will assign only some sort of average lifetime to the system, and the details of the decay rates and their component amplitudes are not immediately apparent. A recurring criticism of the phase technique by those only casually acquainted with the methodology is that multiexponential decays cannot be resolved by phase fluorometry. This outdated criticism is true only if the phase lifetime is taken at a single modulation frequency. As we shall see, when phase and modulation lifetimes are obtained at several frequencies, then multiexponential decays can indeed be resolved.

One can demonstrate (Appendix 2) that a heterogeneous emitting population in the absence of excited state reactions will display an apparent lifetime by phase which is less than the apparent lifetime by modulation. Moreover, the higher the modulation frequency, the shorter will be these measured lifetimes. The relationships for the phase angle, ϕ, and square amplitude, M^2, observed for a mixture of sinusoidally modulated components of phases ϕ_i, modulation M_i, and fractional intensities f_i are given by [38]

$$\tan \phi = \sum_i f_i M_i \sin \phi_i / (\sum_i f_i M_i \cos \phi_i) \tag{9}$$

and

$$M^2 = (\sum_i f_i M_i \sin \phi_i)^2 + (\sum_i f_i M_i \cos \phi_i)^2 \tag{10}$$

Using Weber's notation [38] we can write

$$\tan \phi = S/G \tag{11}$$

$$M^2 = S^2 + G^2 \tag{12}$$

where

$$G = \sum_i f_i M_i \cos \phi_i \tag{13}$$

$$S = \sum_i f_i M_i \sin \phi_i \tag{14}$$

The effect of lifetime heterogeneity on the measured phase and modulation as a function of frequency is illustrated in Fig. 5. This figure gives the calculated phase angle and relative modulation curves for individual lifetime components of 3.1 and 8.7 ns as well as the curves for the corresponding 1:1 mixture (in terms of relative contribution to
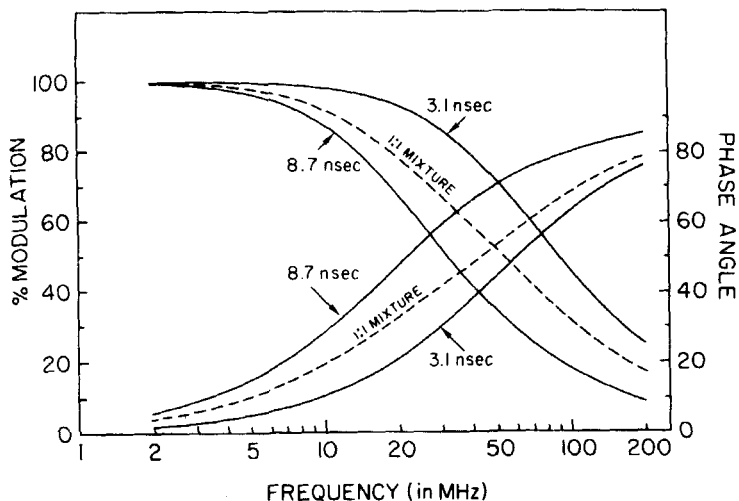

FIG. 5. Simulated multifrequency phase and modulation curves for single exponential decays of 3.1 and 8.7 ns and for a 1:1 mixture of the two components.

the photocurrent). One notes that the phase angle increases as the modulation frequency increases while the relative modulation declines.

Several approaches have been taken to derive the component life-times from the apparent phase and modulation lifetimes obtained at different modulation frequencies. These approaches are discussed in some detail in the following section.

2. Early Approaches

The possibility of using multifrequency phase and modulation measurements to analyze for lifetime heterogeneity has been recog-nized for some time [1, 22] but few examples of such analysis appear in the literature. Schuldiner et al. [39] used phase and modulation data obtained at two frequencies (14.2 and 28.4 MHz) to analyze data for a biochemical preparation (discussed in Section 6). Their analysis pro-cedure consisted essentially of fitting the two frequencies phase and modulation data to Eqs. (9) and (10) utilizing an iterative procedure to find the best fit for the two components lifetimes, τ_1 and τ_2, and their respective fractional contributions, f_1 and f_2.

3. Weber's Algorithm

The closed form, analytical solution for determining N lifetime components and their respective fractional contributions to the total intensity given phase and modulation data at N modulating frequencies has been presented by Weber [38]. The basic operational principles of this procedure are outlined below; the reader is referred to the original article for the rigorous derivation of the algorithm.

Given a circular frequency, ω_r (where $\omega = 2\pi f$ and f represents the linear modulating frequency), one can determine an apparent lifetime by phase, τ_r^P, and an apparent lifetime by modulation, τ_r^M, for a heterogeneous emitting population. In the nomenclature already estab-lished we may express the measured phase shift, ϕ_r, and relative modulation, M_r, as

$$\phi_r = \tan^{-1}(S_r/G_r) \tag{15}$$

$$M_r^2 = S_r^2 + G_r^2 \tag{16}$$

We see then that the G_r and S_r terms are directly related to the com-ponents of the system according to the relations

$$G_r = \sum_i f_i(1 + \omega_r^2 \tau_i^2)^{-1} \tag{17}$$

$$S_r = \sum_i f_i \omega_r \tau_i (1 + \omega_r^2 \tau_i^2)^{-1} \tag{18}$$

where f_i is the fraction of the intensity of the fluorescence detected due to the i-th component and τ_i is the lifetime of the i-th component (note that $\Sigma\, f_i = 1$). In fact, f_i represents the contribution of the i-th component to the detector photocurrent. If f_i is to be related to the chemical composition, i.e., the mole fraction, then one must take into account the relative quantum yields of the various species as well as the relative response characteristics of the detection system to the different emissions. We should also note that the fractional contributions to the steady-state intensity, f_i, is related to the preexponential factors, α_i, commonly given in pulse analysis (Eq. 2) by the relation

$$f_i = \alpha_i \tau_i / (\sum_j \alpha_j \tau_j) \tag{19}$$

where the j index runs over all the contributions to the emission.

For a system of two components one may derive values of G_1, G_2, S_1, and S_2 from the phase (τ_1^P and τ_2^P) and modulation (τ_1^M and τ_2^M) lifetimes at two modulation frequencies, ω_1 and ω_2. One thus obtains

$$G_1 = \{[1 + (\omega_1 \tau_1^P)^2 \; 1 + (\omega_1 \tau_1^M)^2]\}^{-\frac{1}{2}} \tag{20}$$

$$S_1 = G_1 \omega_1 \tau_1^P \tag{20a}$$

The values G_2 and S_2 follow in like fashion. The appropriate arrangement of the G and S terms permits the calculation of the component lifetimes and amplitudes. Again we refer readers to Weber's article for the details of the derivation. The appropriate equations are

$$m_0 = p_1^2 G_1 - p_2^2 G_2 \tag{21}$$

$$m_1 = p_1 S_1 - p_2 S_2 \tag{22}$$

$$m_2 = -G_1 + G_2 \tag{23}$$

$$m_3 = -S_1/p_1 + S_2/p_2 \tag{24}$$

where p_1 and p_2 are small dimensionless numbers given by

$$p_1 = \omega_1/\omega_0 \tag{25}$$

$$p_2 = \omega_2/\omega_0 \tag{26}$$

with ω_0 chosen as a convenient base frequency such as one megahertz.

Weber defines the symmetric functions of the lifetimes as

$$\theta_1 = (m_3 m_0 - m_2 m_1)/m_2 m_0 - m_1{}^2) \tag{27}$$

$$\theta_2 = (m_3 m_0 - m_2{}^2)/(m_2 m_0 - m_1{}^2) \tag{28}$$

The component lifetimes are then given by

$$\frac{\theta_1}{2} \pm (\theta_1{}^2/4 - \theta_2{}^2)^{\frac{1}{2}} \tag{29}$$

where the two roots of the quadratic expression are $\omega_0 \tau_1$ and $\omega_0 \tau_2$.

The fractional contributions may be calculated in many ways, for example:

$$f_2 = [G_1 - (1 + \omega_1{}^2 \tau_1{}^2)^{-1}]/[(1 + \omega_1{}^2 \tau_1{}^2)^{-1} - (1 + \omega_1{}^2 \tau_1{}^2)^{-1}] \tag{30}$$

The solution for N components using N modulating frequencies proceeds along similar lines.

The first study to utilize Weber's algorithm was designed to verify the applicability of the method and to explore the precision and sources of errors inherent in the instrumentation then available [40]. This study concerned the fluorescence of tryptophan as a function of the pH which, under the conditions of the experiments, could be treated as a two-component system. The results indicated that quite good precision was needed to effectively utilize the analytical solution. The results further indicate that standard errors of a few tens of picoseconds in the measured phase and modulation values lead to uncertainties of a few hundred picoseconds in the resolved component lifetimes. The effect is indicated in Fig. 6 which depicts the standard errors expected in the resolved lifetimes for a two-component system ($\tau_1 = 3.1$ ns; $\tau_2 = 8.7$ ns) versus f_1/f_2, the ratio of the fractional intensities. The figure shows the calculated deviations resulting from errors in the phase and modulation lifetimes ($\Delta \tau^P = \Delta \tau^M$) of 100, 50, and 25 ps; the frequencies utilized were 6 and 30 MHz.

A recent study of Weber's algorithm [41] explored the origins of the stringent precision requirements of the method. An interesting result of this study was the finding that the use of more than two frequencies to solve a two-component system can lead to an increase in the uncertainty of the resolved lifetimes. This result was unexpected since one may suppose that knowledge of phase and modulation values at many different frequencies would reduce the uncertainty in the calculated components. The explanation of this effect is based upon the nature of the equations of the analytical solution. In the analytical
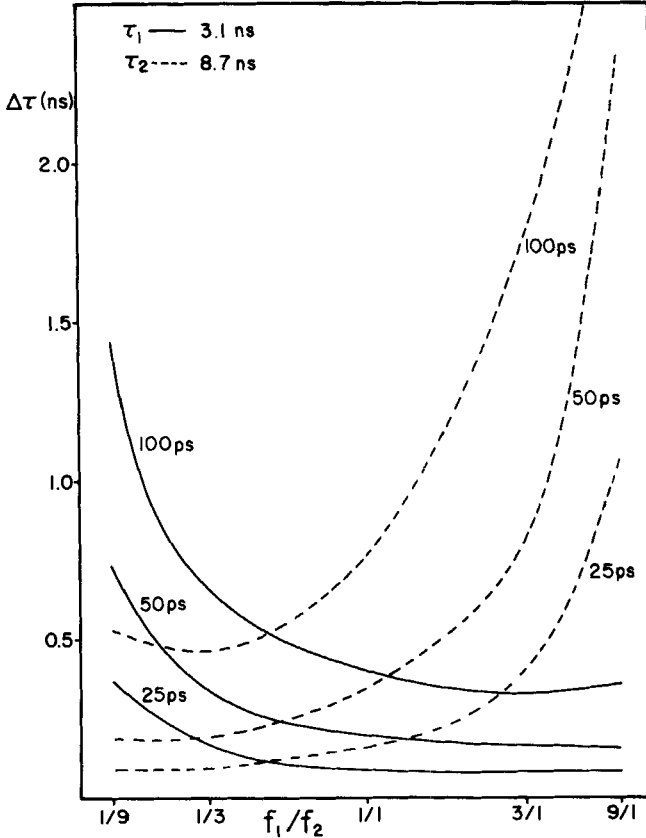
FIG. 6. Expected errors in the derived component's lifetime for
a two-component system of 3.1 and 8.7 ns as a function of the frac-
tional ratio of the components for different assigned errors in the
measured lifetime values using 6 and 30 MHz modulation frequencies
$(\Delta\tau^P = \Delta\tau^M)$.

solution the moments of the distribution of the lifetimes are related to
the experimentally determined functions G_r and S_r through coefficients
Y_{rk} (see Eqs. 13 and 14 of Weber's article [38]). The values of the
coefficients, however, depend upon the set of modulation frequencies
chosen, and one observes that the coefficients for the higher frequencies
are weighted more than for the lower frequencies. This weighting effect
is negligible if the experimental data are of very high precision. In

practice, however, the result can be an amplification of the experimental statistical error which may render the closed form solution practically inapplicable for the case of three or more frequencies given the accuracy of present day instrumentation. Weber's algorithm was an important step, however, since it represents the true analytical solution of the problem. We should also emphasize that the analytical method was developed for applications wherein only a few modulation frequencies were available.

4. Least-Squares Analysis

A different approach was presented by Jameson and Gratton [41]. The basic idea is to use well-known statistical methods for the derivation of the component lifetimes and fractional intensities. A nonlinear least-squares routine was written for an Apple II computer closely following the procedure outlined in Ref. 42. The function to be minimized is defined as

$$F = (1 - w) \sum_r [(\phi_r^c - \phi_r^m)/\sigma_r^\phi]^2 + w \sum_r [(M_r^c - M_r^m)/\sigma_r^M]^2 \quad (31)$$

where ϕ_r^c and M_r^c are the calculated values of phase and modulation, respectively, according to Eqs. 15 and 16 using the relations of Eqs. (17) and (18), ϕ_r^m and M_r^m are the measured values of phase and modulation at frequency ω_r, and σ_r^ϕ and σ_r^M are the experimental errors in the measurements of phase and modulation respectively. The parameter w is a weighting factor. For $w = 1$ only modulation data are computed while for $w = 0$ only phase data are considered. Generally the values of σ_r^ϕ and σ_r^M are independent of the frequency and equal for each measurement, so they factorize out. A normalized quantity used to judge the "goodness" of the fit is defined as

$$\chi^2 = \frac{1}{\sigma^2} F/(\text{number of degree of freedom}) \quad (32)$$

A value of χ close to one indicates good fitting.

The covariance matrix of the errors on the derived parameters (component lifetimes and fractional intensities) is obtained using the procedure given in Ref. 42. Both the diagonal and off-diagonal terms of the error matrix must be considered; the square root of the diagonal terms are the errors in the derived parameters while the off-diagonal terms yield the correlation coefficient among the parameters [42]. A typical list-out of the least squares analysis is shown in Table 1.

The program written for the Apple II computer can resolve up to four independent components. Also, the program allows one to fix the

TABLE 1. List-out of Multifrequency Least-Squares Analysis on a
Two-Component System[a]

Results of 11 successful iterations using phase and modulation
Final chi square = 4.37
Assuming common sigma of 0.2

Component 1 τ = 12.083 ns $\underline{f}$ = 0.534
Component 2 τ = 1.379 ns $\underline{f}$ = 0.466

Analysis of errors
Using average deviation of 0.226

Error on lifetime 1   0.244 ns
Error on fraction 1   0.060
Error on lifetime 2   0.018 ns

Matrix of correlation coefficients

1.000	−0.686	0.663
−0.686	1.000	−0.800
0.663	−0.800	1.000

F	ϕ	ϕ_c	ϕ_{dev}	M	M_c	M_{dev}
1.00	2.500	2.547	−0.047	0.997	0.998	−0.001
1.50	3.822	3.808	0.014	0.996	0.995	0.001
2.00	5.050	5.053	−0.003	0.991	0.992	−0.001
3.00	7.505	7.477	0.028	0.981	0.982	−0.001
5.00	11.986	11.957	0.029	0.952	0.953	−0.001
7.00	15.892	15.816	0.076	0.915	0.915	−0.000
10.00	20.703	20.356	0.347	0.854	0.855	−0.001
15.00	25.568	25.154	0.414	0.762	0.763	−0.001
20.00	27.933	27.802	0.131	0.695	0.694	0.001
30.00	30.846	30.670	0.176	0.611	0.608	0.003
45.00	34.574	34.036	0.538	0.538	0.539	−0.001
70.00	40.344	40.228	0.116	0.470	0.470	−0.000
85.00	42.877	43.945	−1.068	0.434	0.437	−0.003
100.00	47.419	47.433	−0.014	0.422	0.407	0.015
115.00	50.376	50.620	−0.244	0.394	0.379	0.015
140.00	56.414	55.241	1.173	0.358	0.339	0.019

Average ϕ_{dev} = 0.276   Average M_{dev} = 0.004

[a]F = Modulation frequency in MHz. ϕ = Measured value of phase in
degrees. ϕ_c = Calculated values of phase in degrees. ϕ_{dev} = Difference
between calculated and measured values of phase. M = Modulation values.
M_c = Calculated values of modulation. M_{dev} = Difference between cal-
culated and measured values of modulation.

values of some of the parameters and solve for the others. The proce-
dure usually employed consists in first trying a fit using a single com-
ponent. If very large values of χ and systematic deviations of the calcu-
lated phase and modulation values with respect to the measured data
are obtained, then a fit using two components is attempted. In some
particular cases the lifetime of one component is known independently.
The fitting problem is thus simplified and in these cases as many as
three components can be fit successfully.

Recently, an extensive study has been carried out using a mixture
of two fluorophores of known lifetime in order to test the ability of the
method to resolve a double exponential emission. In all cases studied
the values of the component lifetimes and fractional intensities deter-
mined were in very close agreement with the expected results. In
Table 2 we report some representative examples of this unpublished
study. We believe that these experiments demonstrate convincingly the
capability of phase and modulation fluorometry to analyze heterogeneous
emission.

A slightly different least-squares approach has been presented by
Klausner et al. [43]. These researchers used least-squares analysis,
but instead of minimizing the direct observable quantities (phase and
modulation), they chose to use the derived quantities of phase and

TABLE 2

Results of Multifrequency Least-Squares Analysis
on Two-Component Systems[a]

	τ_1	f_1	τ_2
POPOP/9-CA			
Expected values	1.373	0.50	12.327
Measured values	1.378 ± 0.015	0.466 ± 0.005	12.082 ± 0.205
POPOP/9,10-DPA			
Expected values	1.373	0.50	6.417
Measured values	1.470 ± 0.036	0.540 ± 0.018	6.36 ± 0.26

[a]Lifetimes in nanoseconds. Expected values of lifetime were taken
from multifrequency measurements on the pure compounds and steady-
state intensities were calculated from measured intensities of the pure
compound prior to the mixing. Derived values are preliminary results
of a detailed forthcoming analysis (Gratton, Lakowicz, Laczko,
Limkeman, Cherek, and Maliwal, manuscript in preparation).

modulation lifetime. Although in principle this approach should be
equivalent to the one discussed above, in practice different results can
be obtained because of the presence of systematic errors. For example,
as discussed in Section IV-B, color errors can add a small angle to
the expected phase measurement. Under particular circumstances the
color artifact can translate in a large deviation of the phase lifetime
τ^P with respect to the expected value giving an incorrect fit.

5. Other Methods

When phase and modulation values are measured at two frequencies
only, a simplified approach can be used. For example, Visser et al.
[44], using only three of the four measured values (two phase angles
and one modulation ratio), have inverted the expressions given in
Eqs. (17) and (18) with respect to the unknown lifetimes values and
fractional intensities. This approach is clearly an exact solution to be
used for two-component cases when only three experimental data are
available.

IV. INSTRUMENTAL ARTIFACTS

A. General

We may distinguish between several types of instrument-related
artifacts which can affect fluorescence lifetime measurements in gen-
eral and heterogeneity analysis in particular. We shall not discuss
here the more obvious correction factors which take account of the
relative intensity response characteristics of monochromators and
photomultipliers. Rather we shall concentrate on those effects which
are peculiar to time domain measurements. Such considerations are
important since these systematic errors are generally much larger
than the noise in the measurements. As we shall see in our discussion
of heterogeneity analysis, the presence of small systematic errors in
phase or modulation data can have profound effects upon the results.

B. Color Errors

Lifetime measurements are complicated by the well-known [19, 45]
color error which results as a consequence of the systematic increase
in the kinetic energy of the photoelectrons with the energy of the gen-
erating photons. The result of this systematic increase is that the
fluorescence generates a photocurrent that is delayed by a small time
interval, $\Delta\tau_{EL}$, relative to the photocurrent generated by the scattered

photon [40]. For phase measurements this delay translates into an increase, $\Delta\phi_{EL}$, in the phase angle difference between the two photocurrents. $\Delta\phi_{EL}$ and $\Delta\tau_{EL}$ are related by

$$\Delta\phi_{EL} = \omega\Delta\tau_{EL} \tag{33}$$

One thus finds that the measured or technical phase delay, ϕ, and corresponding lifetime, τ^P, for a homogeneous emitting population will depend upon this delay angle as well as on the molecular or electronically undistorted phase delay, ϕ_0, and the associated molecular lifetime, τ_0, according to the relation

$$\tan \phi = \tan (\phi_0 + \Delta\phi_{EL}) = (\tan \phi_0 + \tan \Delta\phi_{EL})/(1 - \tan \phi_0 \tan \Delta\phi_{EL}) \tag{34}$$

Assuming that $\Delta\phi_{EL}$ is small, we have

$$\tau^P = (\tau_0 + \Delta\tau_{EL})/(1 - \omega^2\tau_0\Delta\tau_{EL}) \tag{35}$$

or

$$\tau_0 = (\tau^P - \Delta\tau_{EL})/(1 + \omega^2\tau^P\Delta\tau_{EL}) \tag{36}$$

These equations are the same as those given in Ref. 40 although the starting point is slightly different. Hence we note that a fixed delay, $\Delta\tau_{EL}$, results in a phase lifetime which increases rapidly with τ_0 and ω. This fact owes, of course, to the nature of the tangent function, i.e., an increase of 1° at a nominal phase angle of 45° is not nearly so deleterious as the same 1° increase at a nominal phase angle of 80°.

Table 3, using data from Ref. 40, shows the effect of various electronic delays on the apparent phase lifetime for three frequencies assuming a molecular lifetime of 30 ns. In actual measurements using the EMI 9813QB photomultiplier tube and a fluorophore having a 30-ns lifetime in water (DENS), phase lifetimes corresponding to $\Delta\tau_{EL}$ = 0.5 ns were found. The value of $\Delta\tau_{EL}$ depends, of course, upon the wavelength of excitation and emission. The $\Delta\tau_{EL}$ = 0.5 ns situation corresponded to excitation at 350 nm and observation through a Corning 3-72 cutoff filter which, in the case of this fluorophore, gave an emission centered near 470 nm. By comparison, the Hamamatsu R928 photomultiplier gave no evidence of color error under the same conditions for DENS, i.e., phase lifetimes of 30 ns were observed even up to frequencies of 40 MHz.

TABLE 3

Effect of the Error on the Apparent Phase Lifetime
for a Molecular Lifetime of 30 ns[a]

MHz	$\Delta\tau_{EL} = .5$	$\Delta\tau_{EL} = .94$	$\Delta\tau_{EL} = 1.0$
6	31.16	32.27	32.28
18	37.74	48.34	50.30
30	65.31	—	-470.00

[a]$\Delta\tau_{EL}$ and lifetimes in nanoseconds. $\tau = 30$ ns.

We may note that if the color error is due to a time delay in the photomultiplier, then the modulation lifetime will not be affected. As regards color effects, the modulation measurements offer a distinct advantage over both the phase and the pulse method.

One may circumvent these color errors in several ways such as by using, in place of the scattering solution, a reference compound of known lifetime and spectral distribution similar to the fluorophore. This procedure has been followed for a number of years by the pulse lifetime community. Alternatively, one can determine the $\Delta\tau_{EL}$ for the photomultiplier under the particular conditions of excitation and emission using a plot of the reciprocal of the measured phase lifetime versus the square of the circular modulation frequency which yields $\Delta\tau_{EL}$ as the slope, a procedure outlined in Ref. 40. The best approach, however, would be to utilize a photomultiplier with negligible color error, such as the Hamamatsu R928 or equivalent.

C. Geometrical Effects

Another type of artifact can arise in phase and modulation fluorometry if the modulation of the exciting light is nonhomogeneous with regard to phase and amplitude over the cross section of the beam. The effects of these artifacts in both phase and modulation measurements are discussed in detail in Ref. 34. These effects can be quite dramatic and we illustrate the consequences with the following brief study performed on a conventional SLM 4800A instrument.

After traversing the ultrasonics tank the light is focused on a narrow slit approximately 0.2 mm wide and 1 cm high. With the excitation monochromator set at 500 nm and using 30 MHz modulation

frequency, the exciting beam was divided in half along the vertical axis
at the position of the cuvette holder using an opaque mask. The phase
delay, ϕ, and modulation ratio, M, for a scattering solution were then
measured while masking either the upper or lower half of the beam. A
typical result is shown below.

	Upper	Lower
ϕ	317.7°	298.2°
M	1.691	1.303

When the tank was retuned (using the micrometer adjustment procedure
described earlier), different values of ϕ and M were obtained demon-
strating that the modulation of the beam was nonhomogeneous along the
vertical axis.

The lifetime of a solution of dimethyl POPOP in ethanol at 30 MHz
modulation frequency was measured using the upper part of the beam
for the scatter reference and the lower part for the fluorescence, then
repeating the measurements with the masks reversed and removed
altogether. The results are presented in Table 4. The tank was then

TABLE 4

Effect of Masking Sections of the Exciting Beam
on Phase and Modulation Lifetimes
for Dimethyl-POPOP in Ethanol[a]

Case 1:   Sample-upper<->scatter-lower

$\tau^P = 0.87 \pm 0.03$ ns

$\tau^M = 3.03 \pm 0.02$ ns

Case :   Sample-lower<->scatter-upper

$\tau^P = 2.25 \pm 0.02$ ns

$\tau^M = 0.80 \pm 0.02$ ns

Case 3:   Without mask

$\tau^P = 1.91 \pm 0.01$ ns

$\tau^M = 1.50 \pm 0.01$ ns

---

[a] τ^P = phase lifetime in nanoseconds. τ^M =
modulation lifetime in nanoseconds.

TABLE 5

Effect of Masking Sections of the Exciting Beam
on Lifetime Measurements on Quinine-Bisulfate
in $0.1 \underline{M} H_2SO_4$

	Upper	Lower
$\phi =$	$150°$	$95°$
$M =$	1.039	1.431

Case 3: Without mask

$\tau^P = 21.44 \pm 0.03$ ns

$\tau^M = 19.29 \pm 0.05$ ns

	Upper	Lower
$\phi =$	$112°$	$146°$
$M =$	0.727	0.979

Case 3: Without mask

$\tau^P = 17.46 \pm 0.05$ ns

$\tau^M = 18.38 \pm 0.05$ ns

	Upper	Lower
$\phi =$	$124.6°$	$125.3°$
$M =$	1.633	1.616

Case 3: Without mask

$\tau^P = 19.05 \pm 0.02$ ns

$\tau^M = 18.86 \pm 0.02$ ns

retuned with the aim to match, as well as possible, the phase and mod-
ulation of the upper and lower halves of the beam. The results of the
retuning gave:

	Upper	Lower
ϕ	$280.37°$	$280.33°$
M	1.236	1.239

Repeating Case 3 from Table 4 gave:

$$\tau^P = 1.60 \pm 0.01 \text{ ns}$$

$$\tau^M = 1.24 \pm 0.05 \text{ ns}$$

These results indicate an improvement in the data as a result of the tuning. Similar results for quinine sulfate lifetimes are reported in Table 5. These results also indicate that the measured lifetime values may depend upon the tuning of the ultrasonics tank but that if the criteria of spatial homogeneity of the phase and modulation of the exciting beam is applied, accurate results may be obtained.

V. PHASE-SENSITIVE DETECTION

A. History

        One of the first examples of phase-sensitive detection must be the original experiment of Armand Hippolyte Louis Fizeau [46] who, in 1849, effected terrestrial measurements of the speed of light by observing the occlusion of light using a rotating toothed wheel as a phase sensitive detector. Light passed through the notches of the rapidly rotating toothed wheel and reflected from a mirror located 8633 m away; at the appropriate wheel rotation speed the reflected light could be extinguished by a tooth which meant that the signal was 180° out of phase with its source.
        Various types of phase-sensitive detection or nulling techniques have been applied to fluorescence lifetime measurements for many years (see Ref. 1, for example) but it remained for Veselova et al. [47–49] to utilize phase-nulling techniques to resolve individual components of heterogeneous emission. The basic principle of the technique is as follows: If light with a modulated intensity sinusoidally excites a population of fluorophores composed of species which emit with characteristically different spectra and lifetimes (and hence different phase angles), then observation of the emission with a detector sensitive to the phase angle permits, in principle, the spectral resolution of the different components. This technique enabled Veselova et al. to separate the individual components of a mixture of 3-acetyl-amino-N-methylphthalimide and 3,6-diacetyl-amino-N-phthalimide as well as a mixture of quick-frozen monomeric and aggregate anthracene. Few theoretical or experimental details were given, however, and their work seems to have evoked little interest before the end of the decade.

The commercial availability of phase and modulation instrumentation in recent years, though, has prompted a renewed interest in this area. In the last few years, Lakowicz, Cherek and Balter [50-52], using an SLM 4800 phase fluorometer to which they added a phase-sensitive detector (lock-in amplifier), have elaborated and extended the original work of Veselova et al. These researchers, along with researchers with the spectroscopy firm of SLM-AMINCO [53], have demonstrated the sensitivity and resolving power of the technique when applied to solutions of weak emission intensity and to heterogeneous emission involving small differences in component lifetimes.

B. Technique

In order to convey both the fundamentals of the method as well as its advantages and limitations, we shall give the mathematical description of intensity modulated steady-state heterogeneous emission as a function of the emission wavelength. The total intensity, $S(\lambda, t)$, of the fluorescence emission obtained by a sinusoidally modulated exciting light is given as the sum of the intensity components of the individual species, each with its characteristic phase angle, ϕ_i, and relative modulation, M_i. Thus

$$S(\lambda, t) = \sum_i I_i(\lambda) f_i M_i \sin (\omega t - \phi_i) \tag{37}$$

where $I_i(\lambda)$ describes the unit intensity contribution of the i-th species as a function of the wavelength and f_i the contribution of the i-th species to the total intensity relative to the other contributing species. By definition, $\Sigma f_i = 1$.

The method of phase-sensitive detection consists of multiplying the $S(\lambda, t)$ function by a periodic function $P(t)$ and then integrating the product:

$$PSD = \int_0^T S(\lambda, t) P(t) dt \tag{38}$$

where

$$P(t) \begin{cases} = 0 \text{ from } 0 \text{ to } \phi_D \\ = 1 \text{ from } \phi_D \text{ to } \phi_D + \pi \\ = 0 \text{ from } \phi_D + \pi \text{ to } 2\pi \end{cases} \tag{39}$$
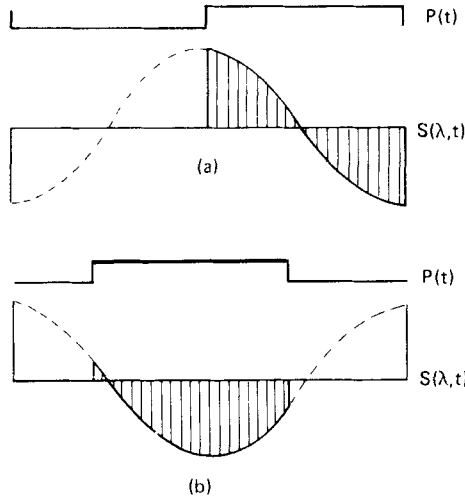
FIG. 7. Waveforms of phase sensitive detection. Case (a): The function $S(\lambda, t)$ is at 90° with respect to $P(t)$. Case (b): The function $S(\lambda, t)$ is at an arbitrary phase angle $\phi_D \neq 90°$.

Carrying out the integration in Eq. (38), we obtain

$$\text{PSD} = \Sigma\, I_i(\lambda) f_i M_i \cos(\phi_D - \phi_i) \tag{40}$$

When $\phi_D - \phi_i = 90°$ or 270°, the intensity contribution of the i-th component to the signal PSD is zero and the observed intensity will be proportional to the contribution of the remaining species.

Figure 7 illustrates the operational principle. Without phase-sensitive detection the electronics will normally isolate the ac component of the signal, rectify it, and determine the average voltage of the complete and rectified signal. The phase-sensitive detector, however, examines only a 180° interval of the unrectified sine wave. Thus, the average voltage detected will be a function of that portion of the sinusoidal signal examined. When the detector "window" is centered around the waveform's maximum and minimum (Fig. 7a), then the average voltage signal consists of a set of component sinewaves originating from different emitting species. Selection of a detector angle which leads to nulling of one component (Fig. 7b) will yield a net voltage corresponding to the contribution of other components out of phase with the nulled component.

In order to select the appropriate detector angle for nulling a spe-
cific component of the emission, the lifetime of that component must
be known. In some cases one can determine the detector angle which
nulls the emission signal at wavelengths where only one component
emits. Alternatively, the mixture can be scanned at several phase
angle settings and the phase-detected signal can be compared with
spectra of the pure components.

Examples of the resolving power of the technique are shown in
Figs. 8 and 9. Figure 8 shows the steady-state spectrum of a 1:1 mix-
ture of anthracene and perylene in methanol. The individual components
of the mixture were resolved (solid lines) when the detector phase angle
was set to be 90° out of phase with one component or the other. The life-
times of the individual components were 4.5 and 5.1 ns for anthracene
and perylene, respectively (the modulation frequency was 30 MHz).
Figure 9 shows a similar experiment using POPOP and dimethyl-
POPOP in ethanol which have lifetimes of 1.0 and 1.2 ns, respectively.
Returning to Eq. (37), we emphasize a limitation of the technique which
has received scant attention in the literature. We have written the equa-
tions for phase-sensitive detection as the sum of many components in
order to focus on the fact that eliminating one intensity component from
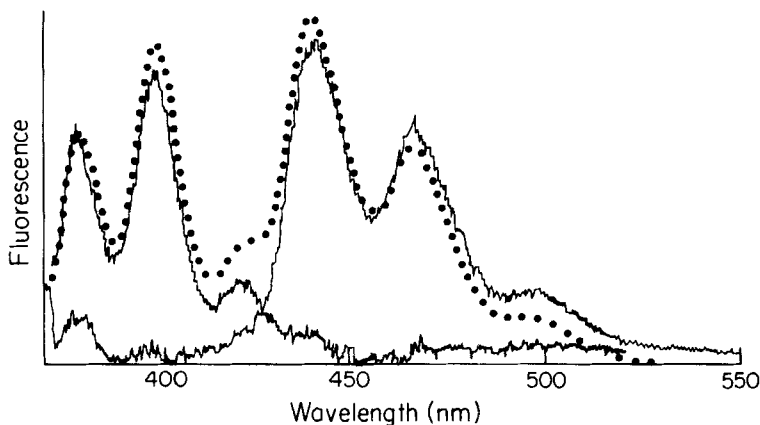the total emission intensity does not guarantee that the remaining signal

FIG. 8. Phase resolved spectra of a mixture of anthracene and
perylene in methanol. Excitation wavelength 361 nm, modulation fre-
quency 30 MHz. Dotted line: Emission spectrum of the mixture. Solid
lines: Phase resolved spectra of the two components. (Reproduced
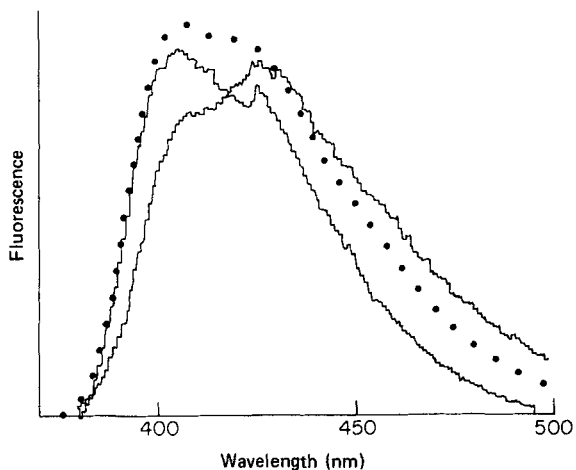with permission from Ref. 53.)

FIG. 9. Phase resolved spectra of a mixture of POPOP and dimethyl-POPOP in ethanol. Excitation wavelength 355 nm, modulation frequency 30 MHz. Dotted line: emission spectrum of the mixture. Solid lines: Phase resolved spectra of the two components. (Reproduced with permission from Ref. 53.)

will correspond to the intensity component of a single species. Most studies to date have concerned well-characterized systems involving only two emitting species. While such model studies have been helpful in demonstrating the resolution capabilities of the technique, the application of phase-sensitive detection to more complex chemical and biological systems threatens to be much more problematic.

A demonstration that a system consists of two components would be the correspondence of the resolved spectra to the spectra expected for the pure components. When even three species contribute to the overall intensity, the results of phase-sensitive detection are difficult to assess and may, in fact, be entirely misleading. In such cases alternative approaches may be utilized. For example, Moya and Garcia [70] and Sebban and Moya [71] have described a method for decomposing fluorescence emission spectra into their elementary components which is based on the simultaneous recording of the fluorescence intensity and apparent lifetime versus the emission wavelength. Phase lifetimes at a particular modulation frequency were obtained; in one case up to seven components in the emission from algae cells at liquid nitrogen temperatures were resolved using a Gaussian fitting procedure.

VI. APPLICATIONS

The use of multifrequency phase and modulation data to resolve heterogeneous emission has not received much attention to date. This dearth of effort owes partly to the general lack of knowledge about the technique, to the fact that rigorous analytical procedures have only recently appeared, and to the very limited availability of true multi-frequency instrumentation. Until recently the heterogeneity analysis using phase and modulation fluorometry could only be applied in particular favorable cases, i.e., two-component systems with well-separated lifetimes or systems in which one or more of the component lifetimes are known independently.

We have already alluded to the early work by Schuldiner et al. [39] who studied the binding of 2-(N-dansyl)aminoethyl-1-thio-β-D-galacto-pyranoside (DG2) to the lac carrier protein of "energized" Escherichia coli membrane vesicles. A homogeneous lifetime of 3.0 ns was observed for the free DG2; after binding to the membrane, however, the lifetime increased and became heterogeneous. The iterative analysis was consistent with a lifetime of 18 ns for the bound DG2 contributing 18% to the total intensity. This analysis was supported by the observed polarization upon binding which was analyzed according to the polarization additivity relationship [54].

A study by Klausner et al. [43] concerned the distribution of the membrane probe DPH in model membrane systems. The results indicated that the DPH lifetime was monoexponential in single-phase vesicles but became heterogeneous in mixed-phase vesicles; these observations were interpreted in terms of a lipid domain model. The data, obtained on a standard SLM instrument at 6, 18, and 30 MHz, were analyzed with a least-squares procedure which we discussed previously. The limited precision of their instrument (standard errors of several hundred picoseconds), coupled with the apparent closeness of the two-component lifetimes, precluded a truly rigorous analysis, and they chose to constrain the two components to 11.1 and 7.4 ns (which correspond to the DPH lifetime in the two isolated single phase systems) and solve for the fractional intensities. A similar study on a more stable and wide range multifrequency instrument would allow, in principle, a more rigorous analysis of such a system but in practice would put a great demand on the present methodology due to the closeness of the component lifetimes.

Another membrane-related study using the same least-squares procedure was carried out by Matayoshi and Kleinfeld [55]. They found that the lifetime of 9-anthroyl-fatty acid membrane probes in egg phosphotidyl vesicles and in nonpolar solvents varied in magnitude and heterogeneity across the emission band. These variations, supported

by polarization studies, were attributed to solvent relaxation effects.
Again the relatively poor precision of the data coupled with the narrow
frequency range studied precludes a completely rigorous analysis of
the system, but their general conclusions indicate that caution must be
exercised when such complex systems are studied by fluorescence
techniques.

A complete spectrofluorimetric characterization, including phase
and modulation lifetime analysis, was performed by Herron and Voss
[56] on 2-dimethylaminonaphthalene-5-sulfonate (DNP) covalently con-
jugated to rabbit IgG antibodies. The lifetime data, taken at 6 and 18
MHz with the fluorometer of Spencer and Weber [22] and analyzed using
Weber's algorithm, indicated near homogeneity of the unconjugated
fluorophore ($\tau = 29$ ns) and the fluorophore conjugated to leucine ($\tau = 22$ ns) yet the existence of two components ($\tau_1 = 30$ ns; $\tau_2 = 3$ ns) upon
conjugation of the fluorophore to normal IgG or purified anti-DNP anti-
bodies. In both antibody systems the long lifetime component contributed
about 87% to the emission. Herron and Voss recognized that the large
errors they obtained for the values of the short lifetime component
could reflect the closed form nature of Weber's algorithm coupled with
the precision of their data. The correspondence between the fractional
intensities and the molar ratios was not clear in the absence of data on
the relative quantum yields of the two forms.

A phase and modulation lifetime study [40] on the pH-dependent
heterogeneous emission of tryptophan using Weber's algorithm was dis-
cussed earlier. We should emphasize that this study was designed to
test the precision of the methodology and not to probe the photophysics
of tryptophan. The results helped to establish that quite high levels of
precision are required for the optimum application of Weber's algorithm
and also served to demonstrate that the precision of an instrument based
on the Debye-Sears effect could be in the range of 30 ps. These data
were subjected to additional scrutiny [41] in a comparison of Weber's
algorithm to a least-squares procedure. In that report a multifrequency
(5, 10, 20, 40, 80 MHz) heterogeneity analysis was also carried out on
a mixture (25%, 75%) of perylene and 9-aminoacridine in ethanol. The
individual components yielded homogeneous lifetimes of 4.33 and 10.99
ns, respectively. Using the least-squares analysis routine, component
values of 3.76 and 10.59 ns were derived in proportions of 26 and 74%,
an agreement which was deemed consistent with the considerations of
the error treatment discussed in the original article.

Another study which utilized Weber's algorithm was that of Sarkar
et al. [57] who investigated the fluorescence lifetime of a partially
purified membrane fraction containing flavin and b-type cytochrome.
Using a standard SLM instrument operating at 10 and 30 MHz, these
researchers obtained the results listed below:

	10 MHz	30 MHz
τ^P	2.887 ns	1.793 ns
τ^M	8.228 ns	4.161 ns

The heterogeneity analysis yielded components of 13.10 and 1.37 ns of fractional weights 30 and 70%, respectively. The major component was assigned to the flavin while the long-lived component was attributed to a porphyrin moiety.

Extensive studies on flavins and flavoproteins have been carried out by Visser and co-workers [44]. Of particular interest is their careful study on pig heart lipoamide dehydrogenase wherein lifetime data obtained by the pulse method (both flashlamp and picosecond laser excitation was used) were compared with that obtained by phase and modulation at 15 and 60 MHz. Both techniques indicated a heterogeneous emission and upon two-component analysis (the phase data were analyzed by a procedure discussed in Section III) gave good agreement in the magnitude of the long component ($\tau = 3.1$ ns at 20°C) whereas the phase method gave a shorter second component than the pulse (0.11 ns compared to 0.54 ns at 20°C) with a greater relative weight (f = 0.76 (phase) compared to f = 0.54 (pulse)).

A phase and modulation study on the quenching by oxygen and acrylamide of the tryptophan fluorescence from horse liver alcohol dehydrogenase was presented by Eftink and Jameson [58]. This dimeric protein contains two tryptophans in each identical subunit. An elegant pulse fluorometry study by Brand and co-workers [59] assigned values of 4.0 and 7.4 ns to the two residues. Since one tryptophan (the long component) was accessible to quenching by acrylamide while the other one was buried and inaccessible, Eftink and Jameson were able to assign the lifetime (3.6 ns) and fractional intensity of the buried residue by observing the lifetime of the protein in the presence of 1 M acrylamide. They were then able to calculate the lifetime of the quenchable component which was consistent with the phase and modulation data in the absence of quencher. The reported lifetimes were 3.6 and 6.9 ns, in reasonable agreement with the pulse results. Simulations were presented in this work of the effect of quenchers on the observed intensity and phase lifetime for a two-component system in which only one component is accessible to the quencher.

An extensive multifrequency phase and modulation fluorometric study was performed on the quenching by oxygen of porphyrin emission from iron-free hemoglobin and myoglobin samples [60, 61]. The results indicated that the emission from these proteins were homogeneous ($\tau = 20.2$ ns for HB^{des} ^{FE}, for example) in the absence of quencher but became markedly heterogeneous as the quencher concentration

increased. The data were obtained in the instrument described in
Section II and were taken at 6, 12, 18, 24, 30, and 36 MHz modulation
frequency. The appearance of heterogeneity in the presence of the
quencher was explained in terms of a theory [61, 62] based on the con-
sideration that the quenching process in proteins requires the penetra-
tion and diffusion of the quencher in the protein matrix as well as a
distribution of quenchers among the protein ensemble.

Ide and Engelborghs [63] have studied the quenching by iodine of
colchicine bound to tubilin using the multifrequency phase fluorometer
previously mentioned [33]. Phase lifetime data were obtained at a num-
ber of modulation frequencies between 1 and 50 MHz. They reported an
homogeneous lifetime of 1.14 + 0.02 ns for colchicine bound to tubilin
at an ionic strength of 0.1 $\underline{M}$ and 1.2 ns at 1 $\underline{M}$. The lifetime data indi-
cated that the quenching by iodine was dynamic with a Stern-Volmer
constant of 5.0×10^8 M^{-1} s^{-1}. The intensity quenching data showed a
marked downward curvature which was interpreted in terms of screen-
ing effect due to the specific ion binding in the neighborhood of the
fluorophore. They also observed that iodine and other chaotropic ions
increased the rate of colchicine release from the complex. Thus life-
time measurements in the presence of iodine were possible with the
phase fluorometer which permitted data acquisition at rates faster than
the kinetics of the system.

Dalbey et al. [73] recently used phase and modulation measure-
ments to determine the distance between two reactive thiols in the heads
of the contractile protein, myosin. Their experiments utilized the energy
transfer between a fluorescent donor (the adduct between a reactive
myosin thiol with 1,5-IAEDANS (N-(iodoacetylaminoethyl)-5-naphthyl-
amine-1-sulfonic acid) and a chromophoric acceptor thiol adduct, (N-
(4-dimethylamino-3,5-dinitrophenyl)maleimide). The donor emission
became heterogeneous in the presence of the acceptor, and the phase
and modulation data obtained on an SLM 4800 at three modulation fre-
quencies, 6, 18, and 30 MHz, were analyzed using an iterative, Monte
Carlo approach. The results were interpreted in terms of a model which
postulates that the two thiols move 6-7 Å closer together upon addition
of Mg ATP. This result is consistent with the author's earlier studies
in which chemical cross-linking of the two thiols was dramatically
enhanced by Mg ATP. The present study demonstrated the possibility
of analyzing for the fractional intensities of a ternary system which
has an appropriate spread of lifetime values, in this case 20.6, 9.3,
and 2.8 ns, when one or two of the lifetime values can be fixed.

VII. CONCLUSIONS

We have discussed the theoretical and practical aspects of phase and modulation measurements as well as the analysis of lifetime heterogeneity, and have demonstrated that the multifrequency approach represents a powerful methodological advance which permits us to realize measurements previously unattainable. Since so much attention in recent years has been focused on the impulse response approach, we may inquire more deeply into the similarities and differences of the impulse and harmonic response techniques. We shall distinguish between the mathematical equivalence of the two methods and the practical differences.

The impulse response and the harmonic response are strictly related for systems which do not exhibit nonlinear (saturation effects, etc.) behavior. The frequency response of the system can be obtained from the pulse response through the use of Laplace transforms. Complete equivalence requires knowledge of the system's response over a wide time and frequency range. The time response is completely determined when the amplitude of the fluorescence signal is measured from times immediately after the pulse to infinitely long times. The frequency response is completely defined when the phase delay and the modulation ratio are measured at all frequencies. The expressions relating the time to the frequency response in terms of the S and G functions are

$$S(\omega) = \int_0^\infty I(t) \sin (\omega t) dt \tag{41}$$

$$G(\omega) = \int_0^\infty I(t) \cos (\omega t) dt \tag{42}$$

where $I(t)$ is the pulse response. The relationship between S and G and the observable phase and modulation values has been given in Eqs. (11) and (12). Knowledge of only one portion of the frequency and time domain renders impossible a direct comparison of the data obtained for the impulse and harmonic response since the integrals in Eqs. (41) and (42) cannot be exactly evaluated. Such a calculation would, however, be an unnecessary exercise since we require to know only the parameters associated with the time response of the system, e.g., the characteristic exponential decay time, τ, in the case of a single exponential decay. The same parameter can be obtained directly from the frequency response without transformation to the time domain. Our purpose, then, is to obtain the parameters of the decay rather than the decay itself.

With this strategy in mind we can implement a procedure in the frequency domain in order to analyze a given fluorescence system. First, we obtain the values of phase and modulation over a significant frequency interval. Second, we calculate the analytical response of the system (the model) directly in the frequency domain. Third, we perform a fit, in the frequency domain, of the desired parameters to the experimentally determined values of phase and modulation. Only at this stage can we make a meaningful comparison of the parameters obtained from the impulse and harmonic methods.

The mathematical equivalence of impulse and harmonic response data does not, however, mean that practical differences between the methods do not exist. One important difference which is seldom mentioned concerns the fact that the impulse response technique does not permit the analysis of photons originating over the complete time domain. The time domain data are in essence truncated and obliged to be between somewhat arbitrary limits in addition to falling into time bins of finite width. In the harmonic response, regardless of the modulating frequency, the time information content of the emitted photons is not sacrificed. Moreover, in the single photon counting pulse technique one is permitted to observe at best only one photon per exciting pulse (to avoid statistical pileup effects this limit is, in fact, reduced) whereas in the harmonic response approach all the photons contribute to the measured signal. This later fact confers a sensitivity to the harmonic method which compares favorably with that of single photon counting, contrary to popular belief.

We may note another misconception about phase fluorometry: that very high frequencies are required for the measurement of nanosecond decays [64]. Although the errors in the phase and modulation measurements show a minimum at a given frequency [65] which depends upon the lifetime, e.g., 1 ns may be most accurately measured near 150 MHz, high precision can still be obtained at much lower frequencies. An arbitrary increase of the frequency will eventually lead to an increase in the error.

Another aspect of the comparison of the impulse and harmonic approach concerns the time required for the measurement. With traditional flashlamp light sources, collection of pulse data of reasonable precision may take many minutes while the actual computer analysis of the results requires an additional period (this point, however, has been recently discussed by Brand et al. [72] who studied the decomposition of a two-component system using a 30-s acquisition period). In contradistinction, phase and modulation data at a single frequency can be obtained in a few seconds while data at several frequencies can be collected in a minute or so. Data analysis is sufficiently rapid to be
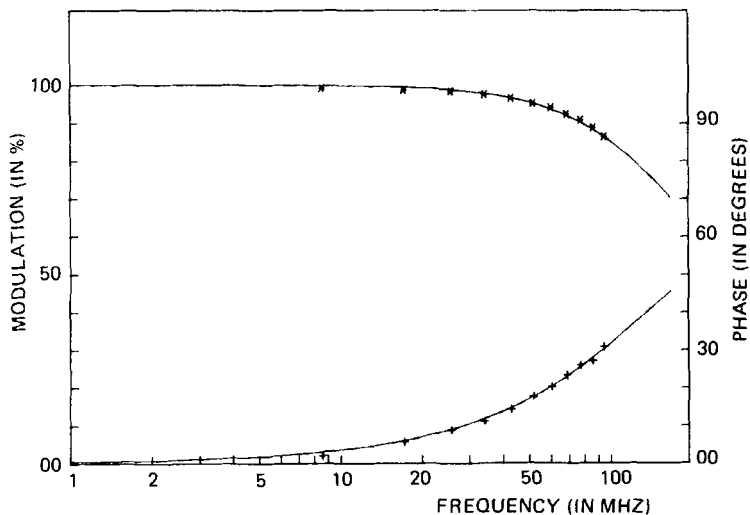
FIG. 10. Multifrequency measurement of phase and modulation
using synchrotron radiation for p-terphenyl in cyclohexane (excitation
at 280 nm, emission observed at wavelength greater than 340 nm).
Modulation (*) and phase (+). The solid lines correspond to a single
exponential decay equal to 980 ps.

performed virtually in real time with the data collection which allows
the experimentalist to monitor a situation closely and to contemplate
kinetic lifetime studies on systems with rate constants in the range
of seconds.

Furthermore, as shown in Section V, the use of phase-sensitive
detection permits one to record directly the individual spectra of two
components with different lifetimes and spectra. Such direct recordings
are not obtainable at present using the impulse method (note that "time
resolved" spectra obtained using single-channel-pulse-height analyzers
to set time windows roughly approximate the true time resolved spectra
but are not equivalent to the direct-phase sensitive recordings).

The phase and modulation approach can, in fact, be coupled with a
high repetition rate pulsed source [66, 67]. Recently a multifrequency
phase and modulation fluorometer has been coupled to the synchrotron
radiation source at the Institute for Nuclear Physics in Frascati, Italy.
This instrument is a virtual replica of the one described in Section II-C
with the exception of the light source. The synchrotron radiation con-
sists of quasi-Gaussian pulses with halfwidths on the order of a nano-

second and a fundamental repetition rate of 8.568 MHz. Data were obtained at the fundamental frequency and each harmonic up to 94.253 MHz. A typical result is shown in Fig. 10. Note that one cannot distinguish between such a measurement done with a pulsed source and that performed using a sinusoidally modulated source.

At the present time multifrequency-phase fluorometry is still at an early stage in development and use. In the near future one may confidently predict the application of the method to a wide range of problems in the physical, chemical, and biological sciences.

APPENDIX 1. DEMONSTRATION OF THE BASIC FORMULAS OF PHASE AND MODULATION FLUOROMETRY

Consider a system described by the following scheme
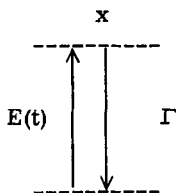
where x is the concentration of the excited state, $E(t)$ the pumping function, and $\Gamma = 1/\tau$ the decay rate.

The differential equation describing this scheme is

$$dx/dt = -\Gamma x + E(t) \qquad (A1)$$

If the pumping function has the form

$$E(t) = E_0(1 + M_E \sin \omega t) \qquad (A2)$$

then the fluorescence emission, which is proportional to x, is given by

$$F(t) = F_0(1 + M_F \sin (\omega t + \phi)) \qquad (A3)$$

Substituting Eq. (A3) in Eq. (A1) and using Eq. (A2), one obtains

$$F_0 M_F \omega (\cos \omega t \cos \phi + \sin \omega t \sin \phi)$$

$$= -\Gamma F_0[1 + M_F(\sin \omega t \cos \phi - \cos \omega t \cos \phi)] + E_0(1 + M_E \sin \omega t)$$
$$\qquad (A4)$$

Because Eq. (A4) must be valid independent of time, the constant term must be zero as well as the coefficients of cos ωt and sin ωt. For the time independent part we have

$$F_0/E_0 = 1/\Gamma \tag{A5}$$

This well-known relation gives the correspondence between fluorescence intensity, excitation, and lifetime.

From the nulling of the cosine coefficient we have

$$F_0 M_F \omega \cos \phi = \Gamma F_0 M_F \sin \phi \tag{A6}$$

which gives the first basic relation of phase fluorometry

$$\tan \phi = \omega/\Gamma \tag{A7}$$

The angle ϕ is called the phase delay or simply the phase of the fluorescence emission.

From nulling the coefficient of the sine term we have

$$F_0 M_F \omega \sin \phi = -\Gamma F_0 M_F \cos \phi + E_0 M_E \tag{A8}$$

Multiplying both sides by cos ϕ we have

$$\omega F_0 M_F \sin \phi \cos \phi + \Gamma F_0 M_F \cos^2 \phi = E_0 M_E \cos \phi \tag{A9}$$

Using Eqs. (A5) and (A6), we can obtain the second basic relation of phase fluorometry:

$$\cos \phi = M_F/M_E \tag{A10}$$

The ratio M_F/M_E is called the modulation ratio or simply the modulation of the fluorescent emission.

Finally, using the tangent expression for the cosine, $\cos \phi = 1/(1 + \tan^2 \phi)^{\frac{1}{2}}$, we can write the two basic relations in terms of phase and modulation:

$$\phi = \tan^{-1} \omega t \tag{A11}$$

$$M = 1/(1 + \omega^2 \tau^2)^{\frac{1}{2}} \tag{A12}$$

where $\tau = 1/\Gamma$.

APPENDIX 2. PHASE AND MODULATION
LIFETIME RELATIONS

We have asserted that a heterogeneous emitting population, in the absence of excited state reaction, will demonstrate a phase lifetime which is always less than the modulation lifetime. The algebraic demonstration of this fact is somewhat cumbersome [11, 68]. We present here a brief and more intuitive demonstration of the phenomenon.

One may make a simple geometrical representation of the phase delay and relative modulation as shown in Fig. 11. Here we depict a vector of length M making an angle ϕ with the x-axis where ϕ represents the phase delay and M the relative modulation. Since for a single exponential decay we have the relation $M = \cos \phi$, the endpoint of the vector is constrained to be on the circle of radius 1/2 with a center at $(1/2, 0)$. The intercept of the extension of this vector with the line through x = 1 equals ωt (since $\tan \phi = \omega t$). This circle is universal for single exponential systems irrespective of the lifetime or modulation frequency. We note that the X and Y intercepts of the vector correspond to our previously defined G and S functions (since $G = M \cos \phi$ and $S = M \sin \phi$).

Figure 12 represents the case of two exponential decays with phase delays and relative modulations of ϕ_1, ϕ_2 and M_1, M_2, respectively. These decays contribute to the total emission intensity decay with fractional weights of f_1 and f_2, respectively. The total fluorescence observed is represented by the vector sum, M, of the two components and gives an observed phase delay of ϕ. Again we see that the intercept of the extension of the M vector with the x = 1 line corresponds to $\omega\tau^P$ (since $\tan \phi = \omega\tau^P$). The value of $\omega\tau^M$, however, corresponds to the line segment BD. This observation follows from the fact that the triangle OAB,
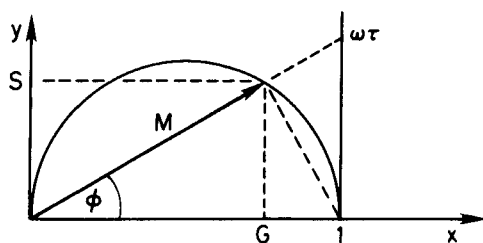

FIG. 11. Geometrical representation of phase delay (ϕ) and modulation ratio (M) for a single exponential decay.

FIG. 12. Geometrical representation of phase delay (ϕ) and modulation ratio (M) for a double exponential decay.

which has a right angle, is congruent to the triangle ODB, which also has a right angle. Hence, from the ratios of the sides we have:

$$DB/BO = AB/DA \tag{A13}$$

Since the side AB corresponds to the quantity $(1 - M^2)^{\frac{1}{2}}$ and OA is equal to M, it follows that

$$DB = (1 - M^2)^{\frac{1}{2}}/M \tag{A14}$$

Since, by definition,

$$\omega\tau^M = (1/M^2 - 1)^{\frac{1}{2}} \tag{A15}$$

we see that DB equals $\omega\tau^M$. Therefore, it is easily recognized in Fig. 12 that in a heterogeneous emitting population τ^P will always be less than τ^M.

APPENDIX 3. CROSS-CORRELATION

The experimental operating principles of cross-correlation phase fluorometry have been discussed in Section II and we present here a

mathematical treatment. When a fluorescent sample is illuminated by light modulated at an angular frequency, $\omega = 2\pi f$, where f is the linear modulation frequency, then the emission can be described by the relation

$$F(t) = F_0[1 + M_F \cos(\omega t + \phi_F)] \qquad (A16)$$

where F(t) is the average fluorescence intensity, M_F the relative modulation, and ϕ_F the phase delay. In the cross-correlation method the emission function is multiplied by a sinusoidal signal of frequency ω_C which is just slightly different from ω, namely:

$$C(t) = C_0[1 + M_C \cos(\omega_C t + \phi_C)] \qquad (A17)$$

where C_0 is the average value of the multiplying function, M_C its relative modulation, and ϕ_C its phase delay. The resulting product signal is the new function

$$V(t) = F_0 C_0[1 + M_F \cos(\omega t + \phi) + M_C \cos(\omega_C t + \phi_C)$$
$$+ M_F M_C \cos(\omega t + \phi) \cos(\omega_C t + \phi_C)] \qquad (A18)$$

Following trigonometric identities, the last term in this equation can be expressed as

$$M_F M_C[\cos(\Delta\omega t + \Delta\phi) + \cos(\omega_C t + \omega t + \Delta\phi)]/2 \qquad (A19)$$

where $\Delta\omega = \omega_C - \omega$ and $\Delta\phi = \phi_C - \phi$. If ω_C is chosen to be very close to ω, then Eq. (A18) contains a constant term plus terms of frequency ω, 2ω, and $\Delta\omega$. The $\Delta\omega$ term contains all the phase and modulation information contained in the original emission signal and can be totally filtered electronically from the remaining terms. The shape of the ac filter which filters the cross-correlation frequency is very important. In fact, as discussed in Ref. 34, the intrinsic nonlinear response characteristics of the modulation system (dynode characteristic, light modulator, amplifiers, etc.) leads to harmonics at $2\Delta\omega$, $3\Delta\omega$, etc. in the low frequency signal. The important consideration is the extent to which these unwanted harmonics influence the measured phase and modulation values. In Fig. 13 we report a calculation of the values of phase and modulation in the presence of a second and third harmonic of an amplitude equal to 1/10 of the fundamental as a function of the phase angle between the fundamental and the harmonic. Deviations from the expected
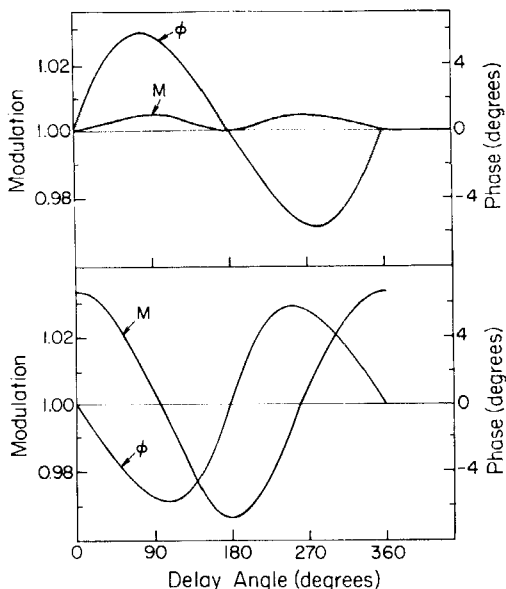
FIG. 13. Effect of a second (upper) and third (lower) harmonic component on observed values of phase and modulation.

values of the phase as large as 6° and from the modulation values as large as 0.03 can result. As a consequence, if an accuracy of 0.1° is required, then the second and the third harmonic must be reduced by the filter by at least a factor of 500 with respect to the fundamental. Depending on the value of the modulation frequency and lifetime of the fluorophore, these deviations can produce dramatic artifacts.

APPENDIX 4. MISCELLANEOUS USEFUL FORMULAS

A. Assume that an emitting system has two forms in equilibrium having lifetimes τ_1 and τ_2 (for example, the case of free and protein-bound ligand). At frequency ω apparent lifetimes by phase and modulation, τ^P and τ^M will be measured. One may derive an expression for the fractional contribution to the photocurrent, f_1 and f_2 (which must then be independently related to the molar quantities as previously described). Using the G and S representation, we find

$$\omega\tau^P = S/G \tag{A20}$$

$$\omega\tau^{M} = [(G^2 + S^2)^{-1} - 1]^{\frac{1}{2}} \tag{A21}$$

where

$$S = f_1\omega\tau_1(1 + \omega^2\tau_1^2)^{-1} + f_2\omega\tau_2(1 + \omega^2\tau_2^2)^{-1} \tag{A22}$$

$$G = f_1(1 + \omega^2\tau_1^2)^{-1} + f_2(1 + \omega^2\tau_2^2)^{-1} \tag{A23}$$

Substitution of Eqs. (A22) and (A23) into Eqs. (A20) and (A21) gives

$$\omega\tau^{P} = [f_1\omega\tau_1(1 + \omega^2\tau_2^2) + f_2\omega\tau_2(1 + \omega^2\tau_1^2)]/[f_1(1 + \omega^2\tau_2^2) + f_2(1 + \omega^2\tau_1^2)] \tag{A24}$$

Solving for the ratio $R = f_1/f_2$:

$$R = \frac{\tau_2 - \tau^{P}}{\tau^{P} - \tau_1} \frac{1 + \omega^2\tau_1^2}{1 + \omega^2\tau_2^2} \tag{A25}$$

This simple expression is useful in the characterization of the extent of reaction when τ_1 and τ_2 are known from independent experiments.

If the assumption that the quantum yields are proportional to the lifetimes is valid (and if the emission spectra of the two species are similar enough so as not to be effected by the response characteristics of the detector system), then the molar ratio, R_m, is given as

$$R_{m} = \frac{\tau_2}{\tau_1} R \tag{A26}$$

An expression similar to Eq. (A25) may be derived for the modulation lifetime, the result being

$$R = \frac{\omega\tau_1 - [(1 + \omega^2\tau_1^2)(1 + \omega^2\tau_2^2)/(1 + (\omega\tau^m)^2) - 1]^{\frac{1}{2}}}{[(1 + \omega^2\tau_1^2)(1 + \omega^2\tau_2^2)/(1 + \omega\tau^m)^2 - 1]^{\frac{1}{2}} - \omega\tau_2} \tag{A27}$$

B. As discussed in Section III, when one examines the phase and modulation lifetimes (for a two-component system) as a function of the modulation frequency, one observes that in the high and low frequency regions phase and modulation lifetimes will reach a constant divergence (Fig. 14). The limiting values of phase and modulation lifetimes are given as
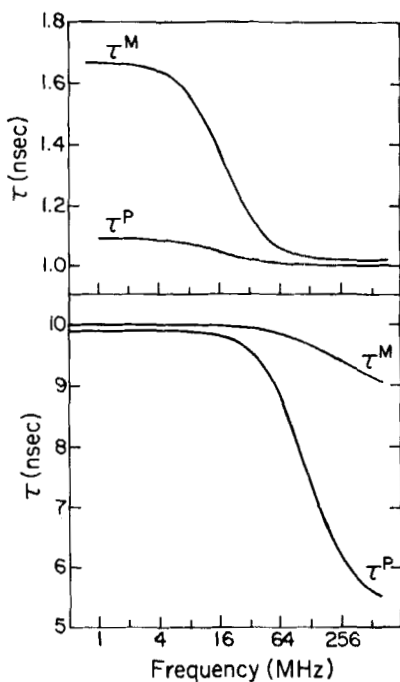
FIG. 14. τ^P and τ^M as functions of the modulation frequency for a two-component system. Upper: $\tau_1 = 10$ ns, $f_1 = 0.01$, and $\tau_2 = 1$ ns. Lower: $\tau_1 = 10$ ns, $f_1 = 0.99$, and $\tau_2 = 1$ ns.

$$\lim_{\omega \to 0} \tau^P = f_1\tau_1 + f_2\tau_2 \tag{A28}$$

$$\lim_{\omega \to \infty} \tau^P = \tau_1\tau_2(f_1\tau_2 + f_2\tau_1)/(f_1\tau_2{}^2 + f_2\tau_1{}^2) \tag{A29}$$

$$\lim_{\omega \to 0} \tau^M = 2(f_1\tau_1{}^2 - f_2\tau_2{}^2)/(f_1\tau_1 + f_2\tau_2) \tag{A30}$$

$$\lim_{\omega \to \infty} \tau^M = \tau_1\tau_2/(f_1\tau_2 + f_2\tau_1) \tag{A31}$$

Teale [11] has also demonstrated that as $\omega \to 0$ the observed phase angle corresponds to the arithmetic mean of the individual phase angle

of the components, whereas when $\omega \to \infty$ the observed modulation corresponds to the arithmetic means of the individual modulations.

C. An interesting effect in the apparent lifetime by modulation has been noted [69] for the case of two components when the fractional contributions and one lifetime are fixed but the other lifetime is varied. Specifically, one can observe an initial decrease and then an increase in τM when the lifetime of one component is increased from zero. The value of τ_2 which gives a minimum in any particular case is given by the derivative of Eq. (12) as

$$(\omega \tau_2)^2 + (2 + f_2/f_1)(1 + \omega^2 \tau_1^2)\tau_2/\tau_1 - 1 = 0 \tag{A32}$$

APPENDIX 5. ELECTRONIC DIGITAL PHASE SHIFTER

The circuit for the electronic digital phase shifter is shown schematically in Fig. 15. At the level of a black box the circuit has two inputs and two outputs. The inputs are a variable (from 4 to 240 MHz) high frequency clock, ck_1, and a fixed (200 Hz) low frequency clock, ck_2. The outputs consist of a frequency, F, equal to the ck_1 input frequency divided by 4 and a frequency $F + \Delta f$ where Δf equals the ck_2 frequency divided by 8. This operation is achieved by the circuit shown in Fig. 15.
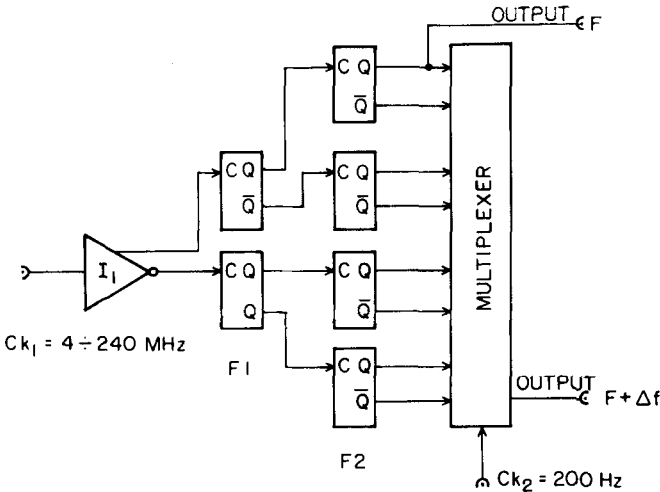

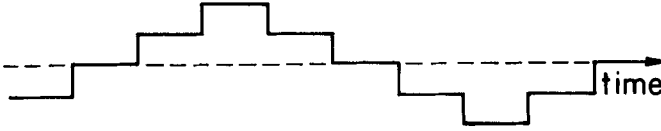FIG. 15. Schematic diagram of the digital phase shifter.

FIG. 16. Low frequency component of the cross-correlation prod-
uct of frequency F and F + Δf generated by the digital phase shifter.

A signal complementary to the ck_1 clock is generated by an inverter
(I1). The two complementary outputs of the inverter, at 180° with re-
spect to one another, are sent to the input of a pair of identical flip-
flops F1. Because the flip-flops are triggered with the positive-going
edge of the clock, after division by two the four outputs of the flip-flops
are shifted by 90°, one with respect to the other. This operation is
repeated by the four identical flip-flops F2 and the 8 corresponding out-
puts are at 45° with respect to one another. At this point the input clock
ck_1 has been divided by 4. The output of any one of the flip-flops F2 is
at a frequency F. The 8 outputs of the F2 flip-flops are multiplexed by
a digital multiplexer in such a way that the multiplexer output advances
by 45° at each step of the multiplexer clock ck_2. The multiplexer output
is the cross-correlation frequency F + Δf. Because in the cross-corre-
lation method only the difference Δf is used, the stability of ck_1 is rela-
tively unimportant. A stability of $1/10^5$ is adequate for ck_2. Using this
technique, the frequency shifting is discrete. Observing the form of the
signal after the product F * (F + Δf) is obtained using a mixer is in-
structive. Two ranges of frequencies are generated, one around 2F and
one around Δf. The residual low frequency signal after removal of the
signal at 2F is shown in Fig. 16. The low frequency signal is composed
of a frequency Δf plus harmonics at 8Δf and higher frequencies. The
signal at Δf must be filtered from the harmonics, an operation accom-
plished by the AC filter already discussed in Section II-B-3.
    The design of the digital phase shifter can be further simplified if
the F2 flip-flops are removed. The operation of the circuit remains
the same. Four steps only are produced, but the circuit operates at
twice the previous frequency, a clear advantage if higher modulation
frequencies are desired.

REFERENCES

[1] J. B. Birks and I. H. Munro, Prog. React. Kinet., 4, 239 (1967).

[2] W. R. Ware, in Creation and Detection of the Excited State, Vol. 1A (A. A. Lamola, ed.), Dekker, New York, 1971, p. 213.

[3] M. G. Badea and L. Brand, Methods Enzymol., 61, 378 (1979).

[4] E. W. Schlag, S. Schneider, and S. F. Fischer, Ann. Rev. Phys. Chem., 22, 465 (1971).

[5] A. J. Roberts, D. V. O'Connors, and D. Phillips, Ann. N. Y. Acad. Sci., 366, 109 (1981).

[6] R. Lopez-Delgado, A. Tramer, and I. H. Munro, Chem. Phys., 5, 72 (1974).

[7] D. M. Jameson and B. Alpert, in Synchrotron Radiation Applied to Biophysical and Biochemical Research (C. Castellani and I. F. Quercia, eds.), Plenum, New York, 1979, p. 183.

[8] A. G. McKinnon, A. G. Szabo, and D. R. Miller, J. Phys. Chem., 81, 1564 (1977).

[9] D. V. O'Connor, W. R. Ware, and J. C. Andre, J. Phys. Chem., 83, 1333 (1979).

[10] B. Valeur, Chem. Phys., 30, 85 (1978).

[11] F. W. J. Teale, in Time Resolved Fluorescence Spectroscopy in Biochemistry and Biology (R. B. Cundall and R. E. Dale, eds.), NATO ASI, Series A, Life Sciences Vol. 69A, Plenum, New York, 1983, p. 59.

[12] E. Gaviola, Ann. Phys. (Leipzig), 81, 681 (1926).

[13] H. Abraham and J. Lemoine, C. R. Acad. Sci. Paris, 129, 206 (1899).

[14] O. Maercks, Z. Phys., 109, 685 (1938).

[15] L. A. Tumerman and V. Szymanovski, Compt. Rend. (Doklady) Acad. Sci. USSR, 15, 323 (1937).

[16] C. F. Ravilious, R. T. Farrar, and S. H. Liebson, J. Opt. Soc. Am., 44, 238 (1954).

[17] E. A. Bailey and G. K. Rollefson, J. Chem. Phys., 21, 1315 (1953).

[18] J. B. Birks and W. A. Little, Proc. Phys. Soc., A66, 921 (1953).

[19] A. Muller, R. Lumry, and H. Kokubun, Rev. Sci. Instrum., 36, 1214 (1965).

[20] A. Schmillen, Z. Phys., 135, 294 (1953).

[21] R. Bauer and M. Rozwadowski, Bull. Acad. Pol. Sci., Ser. Math. Astron. Phys., 7, 765 (1959).

[22] R. D. Spencer and G. Weber, Ann. N. Y. Acad. Sci., 158, 361 (1969).

[23] T. D. S. Hamilton, Proc. Phys. Soc., B70, 144 (1957).

[24] J. B. Birks and D. J. Dyson, J. Sci. Instrum., 38, 282 (1961).

[25] H. P. Haar and M. Hauser, Rev. Sci. Instrum., 49, 632 (1978).

[26] I. Saleem and L. Rimai, Biophys. J., 20, 335 (1977).

[27] H. Gugger and G. Calzaferri, J. Photochem., 13, 21 (1980).

[28] H. Gugger and G. Calzaferri, Ibid., 13, 295 (1980).

[29] G. M. Hieftje, G. R. Haugen, and J. M. Ramsey, Appl. Phys. Lett., 30, 463 (1977).

[30] E. R. Menzel and Z. D. Popovic, Rev. Sci. Instrum., 49, 39 (1978).

[31] H. Merkelo, S. R. Hartman, T. Mar, G. S. Singhal, and Govindjee, Science, 164, 301 (1969).

[32] F. E. Lytle, M. J. Pelletier, and T. D. Harris, Appl. Spectrosc., 33, 28 (1979).

[33] G. Ide, Y. Engelborghs, and A. Persoons, Rev. Sci. Instrum., 54, 841 (1983).

[34] E. Gratton and M. Limkeman, Biophys. J., 44, 315 (1983).

[35] P. Debye and F. W. Sears, Proc. Natl. Acad. Sci., Washington, 18, 410 (1932).

[36] R. D. Spencer and G. Weber, J. Chem. Phys., 52, 1654 (1970).

[37] F. Dushinsky, Z. Phys., 81, 7 (1933).

[38] G. Weber, J. Phys. Chem., 85, 949 (1981).

[39] S. Schuldiner, R. D. Spencer, G. Weber, R. Weil, and H. R. Kaback, J. Biol. Chem., 250, 8893 (1975).

[40] D. M. Jameson and G. Weber, J. Phys. Chem., 85, 953 (1981).

[41] D. M. Jameson and E. Gratton, in New Directions in Molecular Luminescence (D. Eastwood, ed.), ASTM STP 822, American Society for Testing and Materials, Philadelphia, 1983, p. 67.

[42] S. Brandt, in Statistical and Computational Methods in Data Analysis, 2nd ed., North-Holland, Amsterdam, 1976.

[43] R. D. Klausner, A. M. Kleinfeld, R. L. Hoover, and M. J. Karnovsky, J. Biol. Chem., 255, 1286 (1980).

[44] A. J. W. G. Visser, H. J. Grande, and C. Veeger, Biophys. Chem., 12, 35 (1980).

[45] D. M. Rayner, A. E. McKinnon, A. G. Szabo, and P. A. Hackett, Can. J. Chem., 54, 3246 (1976).

[46] A. Fizeau, C. R. Acad. Sci. Paris, 31, 90 (1849).

[47] T. V. Veselova, A. S. Cherkasov, and V. I. Shirokov, Opt. Spectrosc., 29, 617 (1970).

[48] T. V. Veselova, L. A. Limareva, and A. S. Cherkasov, Izv. Akad. Nauk SSSR, Bull. Phys. Ser., 29, 1340 (1965).

[49] T. V. Veselova and V. I. Shirokov, Akad. Nauk SSR, Bull. Phys. Ser., 36, 925 (1972).

[50] J. R. Lakowicz and H. Cherek, J. Biol. Chem., 256, 6348 (1981).

[51] J. R. Lakowicz and H. Cherek, J. Biochem. Biophys. Methods, 5, 19 (1981).

[52] J. R. Lakowicz and A. Balter, Photochem. Photobiol., 36, 125 (1982).

[53] J. R. Matteis, G. W. Mitchell, and R. D. Spencer, in New Directions in Molecular Luminescence (D. Eastwood, ed.), ASTM STP 822, American Society for Testing and Materials, Philadelphia, 1983, p. 177.

[54] G. Weber, Biochem. J., 51, 145 (1952).

[55] E. D. Matayoshi and A. M. Kleinfeld, Biophys. J., 35, 215 (1981).

[56] J. Herron and E. W. Voss, Jr., J. Biochem. Biophys. Methods, 5, 1 (1981).

[57] H. K. Sarkar, P-S. Song, T-Y. Leong, and W. R. Briggs, Photochem. Photobiol., 35, 593 (1982).

[58] M. R. Eftink and D. M. Jameson, Biochemistry, 21, 4443 (1982).

[59] J. B. A. Ross, C. J. Schmidt, and L. Brand, Ibid., 20, 4369 (1981).

[60] D. M. Jameson, M. Coppey, B. Alpert, and G. Weber, Biophys. J., 33, 300a (1981).

[61] D. M. Jameson, B. Alpert, E. Gratton, and G. Weber, Ibid., in press.

[62] E. Gratton, B. Alpert, D. M. Jameson, and G. Weber, Ibid., in press.

[63] G. Ide and Y. Engelborghs, J. Biol. Chem., 256, 11684 (1981).

[64] G. M. Hieftje and G. Horlich, Am. Lab., Issue 76 (March 1981).

[65] E. Gratton and R. Lopez-Delgado, Nuovo Cimento, 56B, 110 (1980).

[66] A. P. Sabersky and I. H. Munro, in Picosecond Phenomena (C. V. Shank, ed.), Springer, New York, 1979.

[67] E. Gratton and R. Lopez-Delgado, Rev. Sci. Instrum., 50, 789 (1979).

[68] R. D. Spencer, PhD Thesis, University of Illinois, 1970.

[69] D. M. Jameson, in Time Resolved Fluorescence Spectroscopy in Biochemistry and Biology (R. B. Cundall and R. E. Dale, eds.), NATO ASI, Series A, Life Sciences Vol. 69A, Plenum, New York, 1983, p. 623.

[70] I. Moya and R. Garcia, Biochim. Biophys. Acta, 722, 480 (1983).
[71] P. Sebban and I. Moya, Ibid., 722, 436 (1983).
[72] L. Brand, J. B. A. Ross, and W. R. Laws, Ann. N. Y. Acad. Sci., 366, 197 (1981).
[73] R. E. Dalbey, J. Weiel, and R. G. Yount, Biochemistry, 22, 4696 (1983).